Research Square

Preprints are preliminary reports that have not undergone peer review.
They should not be considered conclusive, used to inform clinical practice,
or referenced by the media as validated information.

Formaldehyde Inhalation Reduces Regional Parvalbumin Immunoreactivity and Modulates Glial Activation in the Rat Brain

Ifukibot Levi Usende

ifukibot.usende@uniabuja.edu.ng

University of Abuja

Bashir Abdullahi Muhammad

University of Abuja

Idris Nurudeen Abdullahi

University of Abuja

Mobolaji Abdulateef Ayoola

University of Abuja

James Clinton Shawulu

University of Abuja

Fatima Oyelowo-Abdulraheem

University of Abuja

Usende Ephraim Utopejit

University of Abuja

Shurhabilu Ja'afar

University of Abuja

Edem Ekpenyong Edem

Afe Babalola University

Research Article

Keywords: Formaldehyde, Parvalbumin Neurons, Glial Activation, Anatomy Dissection, Occupational Safety, Oxidative Stress

Posted Date: July 24th, 2026

DOI: https://doi.org/10.21203/rs.3.rs-10405857/v1

License: This work is licensed under a Creative Commons Attribution 4.0 International License.
Read Full License

Additional Declarations: No competing interests reported.

Version of Record: A version of this preprint was published at BMC Neuroscience on October 30th, 2026. See the published version at https://doi.org/10.1186/s12868-026-01064-9.

Formaldehyde Inhalation Reduces Regional Parvalbumin Immunoreactivity and Modulates Glial Activation in the Rat Brain

Usende Ifukibot Levi[1]*, Abdullahi Bashir Muhammad[1]; Idris Nurudeen Abdullahi[1]; Mobolaji Abdulateef Ayoola[1]; Shawulu James Clinton[1]; Oyelowo-Abdulraheem Fatima[1]; Usende Ephraim Utopejit[2]; Ja'afar Shurhabilu[1] and Edem Ekpenyong Edem[3]

[1]Department of Veterinary Anatomy, Faculty of Veterinary Medicine, University of Abuja, Abuja, Federal Capital Territory, Nigeria

[2] College of Health Sciences, University of Abuja, Abuja, Nigeria

[3]Department of Human Anatomy, College of Medicine and Health Sciences, Afe Babalola University, Ado-Ekiti, Nigeria.

*Corresponding Authors: ifukibot.usende@uniabuja.edu.ng

Abstract

Formalin is the principal fixative used in gross anatomy dissection, and its vapour (formaldehyde) constitutes a recognized occupational hazard for anatomists, technicians, and students during prolonged cadaveric exposure. While the respiratory and mucosal effects of formaldehyde inhalation are well documented, its impact on the brain's cellular architecture, particularly on fast-spiking, parvalbumin-expressing interneurons that regulate cortical and hippocampal network activity, remains poorly characterized under a chronic, inhalation-based, occupationally relevant exposure paradigm. This study examined the neuroanatomical consequences of 28-day formaldehyde inhalation in adult male Wistar rats. Exposed animals showed a significant, time-dependent decline in body weight gain, a reduction in absolute brain weight, and an elevation in brain formaldehyde concentration relative to controls. Neurobehavioral testing revealed impaired motor coordination, spatial memory, and exploratory behaviour. Formaldehyde-exposed brains showed significantly elevated lipid peroxidation and depleted antioxidant enzyme activities. Immunohistochemical and stereological analysis revealed a marked, region-dependent reduction in the number and soma size of parvalbumin-expressing interneurons in the cerebellar Purkinje layer, hippocampal CA1 region, and cerebral cortex, accompanied by pronounced astrocytic and microglial activation across these regions and the olfactory bulb. These findings indicate that chronic formaldehyde inhalation produces measurable, region-specific neurodegeneration and neuroinflammation in a rodent model that closely mirrors occupational exposure conditions in anatomy dissection settings. The results underscore the need for stricter formaldehyde exposure controls in anatomical education and raise concern regarding the long-term neurological safety of personnel routinely exposed to formalin vapour in dissection halls.

Keywords: Formaldehyde, Parvalbumin Neurons, Glial Activation, Anatomy Dissection, Occupational Safety, Oxidative Stress

Introduction

Gross anatomy dissection remains an irreplaceable pillar of veterinary, medical and health sciences education, and formalin, an aqueous solution of formaldehyde, is still the fixative of choice for cadaver preservation in most anatomy departments worldwide. This near-universal reliance on formalin means that anatomists, laboratory technicians, and generations of medical students are routinely exposed to formaldehyde vapour throughout their training and careers. The scale of this exposure is not trivial: personal breathing-zone concentrations recorded in gross anatomy laboratories have repeatedly exceeded international occupational ceiling limits, with reported levels ranging from below 1 ppm to over 3 ppm depending on ventilation and dissection stage (Chia et al., 1992; Akbar-Khanzadeh et al., 1994; Keil et al., 2001; Vohra, 2011). On the basis of sufficient evidence of nasopharyngeal carcinogenicity in humans and experimental animals, the International Agency for Research on Cancer classified formaldehyde as a Group 1 human carcinogen in 2004 and subsequently extended this classification to leukaemia (IARC, 2006, 2012). Beyond its established links to nasopharyngeal cancer and respiratory irritation, occupational exposure has also been associated with genotoxic effects, including elevated micronucleus frequency and DNA damage in peripheral lymphocytes of exposed anatomy and pathology staff, with the magnitude of damage correlating with cumulative years of exposure (Orsière et al., 2006; Costa et al., 2008; Souza & Devi, 2014). What is far less understood and considerably underexamined in the neuroscience and anatomical sciences literature is how this chronic, low-to-moderate-dose inhalational exposure affects the brain itself, particularly at the level of individual, functionally specialized neuronal populations.

Exposure measurements from anatomy teaching facilities show that a concentration recorded at a fixed room location may underestimate the dose received in the breathing zone of a person leaning over a cadaver. Personal sampling studies have reported exposure concentrations above recommended ceiling or action values during dissection, whereas local exhaust systems and redesigned dissection tables can substantially reduce ambient concentrations (Akbar-Khanzadeh et al., 1994; Coleman, 1995; Keil et al., 2001; Ohmichi et al., 2006; Vohra, 2011). Biomonitoring studies have also reported chromosomal and DNA damage among anatomy and pathology laboratory personnel, supporting the need to evaluate formaldehyde as a multisystem occupational toxicant rather than solely as a mucosal irritant (Orsière et al., 2006; Costa et al., 2008; Souza & Devi, 2014).

The neurotoxic potential of formaldehyde is not in serious doubt because formaldehyde readily crosses the blood-brain barrier. Inhaled or systemically administered formaldehyde has been shown to accumulate in brain tissue and to disrupt learning and memory in rodents, with particular vulnerability in the hippocampus and prefrontal cortex (Gurel et al., 2005; Zararsiz et al., 2007; Aslan et al., 2006). These effects are widely attributed to formaldehyde's capacity to overwhelm endogenous antioxidant defences, generating excess reactive oxygen species that damage neuronal membranes, proteins, and DNA (Tang et al., 2013). Formaldehyde is not, however, purely an exogenous insult: it is also generated continuously as a by-product of normal one-carbon and amine metabolism in the brain, and hippocampal formaldehyde concentration rises with age and has been linked to age-dependent memory decline, indicating that the brain's intrinsic capacity to detoxify formaldehyde is finite and can be overwhelmed by an additional exogenous source (Tulpule & Dringen, 2013; Tong et al., 2013). This convergence of an endogenous metabolic burden with a superimposed, occupationally relevant exogenous exposure strengthens the plausibility that chronic inhalational formaldehyde could produce cumulative, region-specific neuronal injury rather than a transient physiological

perturbation (Songur et al., 2010). What has received comparatively little attention, however, is the differential vulnerability of specific neuronal subtypes to this oxidative burden. Fast-spiking, parvalbumin-expressing GABAergic interneurons are of particular concern in this regard. These cells maintain exceptionally high rates of oxidative metabolism to sustain their rapid firing and central role in coordinating cortical and hippocampal network synchrony, and this same metabolic demand appears to render them disproportionately sensitive to oxidative and redox imbalance relative to other neuronal populations (Steullet et al., 2017). Experimental work in other models of developmental and metabolic stress has shown that glutathione depletion and oxidative insult selectively compromise parvalbumin interneuron integrity and connectivity, with consequences for network function that extend well beyond the cells directly affected (Cabungcal et al., 2006). Whether this same selective vulnerability holds under chronic formaldehyde exposure, and whether it varies systematically across brain regions, has not been directly established.

A further dimension of formaldehyde neurotoxicity concerns its interaction with the brain's immune architecture. Oxidative damage to neurons rarely occurs in isolation; it typically triggers a secondary wave of glial activation, in which astrocytes and microglia shift from their surveillance state into a reactive, hypertrophic phenotype characterized by increased glial fibrillary acidic protein and ionized calcium-binding adaptor molecule 1 expression, respectively (Sofroniew & Vinters, 2010; Kettenmann et al., 2011). This glial response, while initially protective, can become a self-sustaining source of regional neurodegeneration when the inciting insult is prolonged, as with continuous occupational-style exposure rather than a single acute dose. Microglia can initiate inflammatory signals that convert astrocytes into a neurotoxic, so-called A1 reactive phenotype that loses its normal supportive functions and instead promotes the death of neurons and oligodendrocytes, a mechanism now implicated across several chronic neurodegenerative conditions (Liddelow et al., 2017). Concurrent

assessment of GFAP and IBA1 is therefore useful for distinguishing a localized neuronal alteration from a broader neuroinflammatory response distributed across interconnected brain regions.

Parvalbumin-positive neurons combine rapid firing with dense mitochondrial activity and a central role in gamma-frequency synchronization, making them among the most metabolically demanding components of cortical and hippocampal networks (Sohal et al., 2009; Cardin et al., 2009; Kann & Kovács, 2007; Hu et al., 2014). This high energy expenditure is met by an unusually high mitochondrial and cytochrome c oxidase content, a design that leaves these interneurons with a correspondingly narrow margin of tolerance whenever oxidative phosphorylation is challenged by metabolic or oxidative stress (Kann, 2016). Experimental redox disruption reduces PV immunoreactivity and gamma oscillatory function in a manner that can be reproduced pharmacologically, for example, by NADPH-oxidase-mediated superoxide generation following ketamine administration, whereas perineuronal nets, the specialised extracellular matrix that ensheaths mature PV interneurons, provide only partial protection against this oxidative injury (Behrens et al., 2007; Steullet et al., 2010; Cabungcal et al., 2013). These observations provide a mechanistic basis for testing whether formaldehyde-related oxidative stress preferentially alters PV-expressing neuronal populations across brain regions that differ in baseline metabolic demand.

The existing literature, therefore, establishes three separate facts without yet connecting them: that formaldehyde is neurotoxic and readily reaches the brain even at occupationally realistic exposure levels; that parvalbumin interneurons are, on independent mechanistic grounds, plausible candidates for selective vulnerability to oxidative insult; and that sustained oxidative damage recruits a self-amplifying glial response. What remains missing is a study that brings these three threads together within an exposure paradigm designed specifically to model the conditions that anatomists and their students actually experience: chronic, low-dose inhalation

of formaldehyde vapour, rather than the intracerebroventricular, intraperitoneal, or acute high-dose exposures that have dominated the rodent literature to date. Characterizing the regional distribution of parvalbumin interneuron loss and its accompanying glial response under this occupationally relevant paradigm would provide a more direct anatomical and physiological basis for evaluating the neurological risk faced by those who work routinely with formalin-preserved tissue, and would extend the neuroscience and anatomical sciences literature on formaldehyde beyond its traditional focus on respiratory and mucosal endpoints. The present study was therefore designed to examine the effects of 28-day formaldehyde inhalation on body weight, brain weight, neurobehavioral performance, oxidative stress markers, and the regional distribution and morphology of parvalbumin-expressing interneurons and glial populations across different brain regions and olfactory bulb of adult male Wistar rats.

Materials and Methods

Animals and housing

Fourteen (14) adult male Wistar rats (170 ± 0.76 g) were obtained from the Animal Core Facility, Faculty of Veterinary Medicine, University of Abuja, Nigeria, and housed in ventilated cages at the Animal Facility of the Neuroscience Unit, Department of Veterinary Anatomy, University of Abuja. Animals were acclimatized for two weeks before the start of the experiment. They were maintained on a 12-hour light/12-hour dark cycle at an ambient temperature of 20–26 °C and relative humidity of 40–70% throughout the study, with rat chow and clean tap water provided ad libitum. All experiments were performed under veterinary supervision, and every effort was made to minimize the number of animals used and to avoid animal suffering.

Experimental Design

Animals were randomly assigned to two groups of seven animals each. Group 1 served as the control and was exposed to inhaled distilled water vapour, while Group 2 was subjected to

inhaled formaldehyde vapour. Both groups underwent their respective exposure protocols for 28 consecutive days. Group allocation was concealed from the experimenters responsible for behavioural scoring and quantitative histological analysis, thereby minimizing bias in outcome assessment.

Ethical Approval

All experimental procedures were conducted in strict accordance with internationally accepted standards for animal research, specifically the NIH Guide for the Care and Use of Laboratory Animals (NIH Publication No. 8023) and the European Communities Council Directive of 24 November 1986 (86/609/EEC). Ethical clearance was obtained from the University of Abuja Ethics Committee for Animal Use under approval number UAECAU/2022/0018. Every effort was made to minimize animal suffering and to reduce the number of animals used, in line with the principles of humane research practice. The design and reporting of the experiment were evaluated against the ARRIVE 2.0 essential recommendations, including identification of the experimental unit, allocation procedures, blinding, inclusion and exclusion criteria, outcome measures, and statistical methods (Percie du Sert et al. 2020). The individual animal was treated as the experimental unit for all inferential analyses.

Formaldehyde inhalation exposure

The formaldehyde inhalation protocol was adapted from Liu et al. (2010). Formaldehyde vapour was generated by evaporation from a stock formalin solution (≥36%; Sigma-Aldrich, USA) applied to the lower inner surfaces of a static toxification chamber (40 × 40 × 25 cm), yielding a chamber concentration of 10.2 ± 2.1 ppm, verified using a calibrated formaldehyde detector (Forensics Detectors, USA). Rats in the formaldehyde-inhalation group were exposed once daily for 30 minutes (08:00–08:30) for 28 consecutive days. Control animals underwent an identical daily 30-minute exposure protocol in the same chamber type with fresh air only. Chambers were cleaned between successive exposure sessions.

Clinical observation

Body weight was recorded daily using a digital scale (Camry, China). All animals were observed for clinicopathological signs of toxicity 2 hours before, during, and 2 hours after each daily inhalation session.

Neurobehavioral assessment

Neurobehavioral testing was performed after the 28-day exposure period using the forelimb grip strength (hanging wire) test, a modified Morris water maze test, and the open field test, each of which is described below. Two experimenters, blinded to group allocation, independently scored all behavioural outcomes.

Forelimb grip strength (hanging wire) test

Muscular strength and balance were assessed as previously described (Usende et al., 2024; Folarin et al., 2016). Each rat's forepaws were placed on a horizontally suspended wire (2 mm diameter, 1.0 m length) positioned 15 cm above a soft bedding-filled surface to allow safe landing. Latency to fall, the time each animal remained suspended before falling, was recorded using an electronic stopwatch by two experimenters blinded to group allocation. Each animal underwent two trials, followed by a 3-minute rest period before removal.

Modified Morris water maze test

Hippocampal-dependent spatial learning and memory were assessed using a modified Morris water maze protocol (Usende et al., 2024; Folarin et al., 2016; Shabani et al., 2012). The pool (120 cm diameter, 45 cm height) was divided into four quadrants (north, south, east, west), with a hidden circular escape platform (15 cm diameter) placed in a fixed quadrant throughout training. Each animal was gently introduced into the pool and given up to 60 seconds to locate the hidden platform; animals that failed to do so within this time were guided to the platform and allowed to remain there for 15 seconds before removal to a dry holding cage. All animals underwent three training trials per day over two consecutive days. On the third day, a single-

probe trial was conducted with the platform removed, and the latency to reach the former platform location was recorded as a measure of spatial memory retention. Testing was recorded using a video camcorder (Nikon Coolpix L341, Nikon Imaging, USA) mounted 90 cm above the centre of the pool and connected to a laptop computer (Acer Aspire 5, A517-53-54N6) for video capture; all sessions began at 08:00 daily.

Open-field test

Exploratory and anxiety-like behaviours were assessed using a modified open-field protocol as described by Brown et al. (1999) and further adapted by Usende et al. (2016, 2024). The test was conducted on the day of sacrifice. The arena consisted of a glossy white plywood enclosure measuring 64 × 64 × 30 cm, with the floor divided into sixteen 16 × 16 cm grid squares marked in green and a central square of the same size marked in red. Each rat was placed at the centre of the arena and allowed to explore freely for five minutes. Behavioural sessions were recorded using a camcorder mounted 60 cm above the centre of the arena, consistent with the previously described setup.

Between successive trials, the arena was cleaned with 70% ethanol and air-dried for one to two minutes to eliminate olfactory cues. Behavioural scoring was performed according to the parameters outlined by Brown et al. (1999) and modified by Usende et al. (2016, 2024). These included the number of line crossings, defined as instances where the animal crossed a grid line with all four paws; the frequency of rearing, recorded when the animal stood upright on its hind limbs; the total number of faecal boli deposited during the session; and the number of urine puddles or streaks observed.

Sacrifice, tissue collection, and processing

Following completion of behavioural testing, animals were euthanized by lethal injection of xylazine (10 mg/kg) and ketamine (100 mg/kg) (Usende et al., 2016) and transcardially perfused with normal saline for 2 minutes to clear blood from the vasculature. Brains were

dissected on ice, weighed (Lark Electronic Balance, LP 502A, China), and divided into two hemispheres. One hemisphere was immediately processed for biochemical and formaldehyde quantification analyses: tissue was rinsed in 1.15% KCl, homogenized in 0.1 M potassium phosphate buffer (pH 7.4), and centrifuged at 10,000 rpm for 20 minutes. The resulting post-mitochondrial fraction (PMF) supernatant was collected and stored at −20 °C until analysis (Oyagbemi et al., 2017). The contralateral hemisphere was immersion-fixed in 4% paraformaldehyde in 0.1 M PBS for 48 hours, then subjected to immunohistochemical analysis.

Biochemical assessment of oxidative stress and antioxidant markers

Lipid peroxidation was assessed by measuring malondialdehyde (MDA) content in the PMF supernatant, expressed as mmol MDA per mg protein, using the method of Varshney and Kale (1990) with a molar extinction coefficient of 1.56×10^5 $M^{-1}cm^{-1}$ (Oyagbemi et al., 2017). Catalase (CAT) activity was measured by monitoring the rate of hydrogen peroxide decomposition at 240 nm, following a modified method of Oyagbemi et al. (2017). Superoxide dismutase (SOD) activity was determined by assessing inhibition of epinephrine auto-oxidation at pH 10.2 (Misra & Fridovich, 1972). Glutathione-S-transferase (GST) activity was assessed via conjugation of reduced glutathione with 1-chloro-2,4-dinitrobenzene (CDNB), following the method of Habig et al. (1974). Reduced glutathione (GSH) content was measured using the method of Beutler et al. (1963), based on the reaction with 5,5′-dithiobis (2-nitrobenzoic acid) (DTNB) to produce a yellow chromophore.

Quantification of brain formaldehyde concentration

Brain formaldehyde concentration was determined in the PMF supernatant by gas chromatography-mass spectrometry (GC-MS) following derivatization with 2,4-dinitrophenylhydrazine (2,4-DNPH) to form the formaldehyde-DNPH (FA-DNPH) derivative, as described by Kleinnijenhuis et al. (2012). A 2,4-DNPH stock solution was prepared by combining 0.01 g DNPH and 0.1 mL concentrated H_2SO_4 in a 50 mL volumetric flask, brought

to volume with acetonitrile. Working standards of FA-DNPH were prepared at 0.2, 0.5, 1.0, 2.0, 5.0, 10, 20, and 50 mg/L by serial dilution of the reference standard. GC-MS analysis was performed using a nitrogen carrier gas at 1 mL/min, a 10:1 split ratio, and an injection volume of 0.6 µL. The injection port temperature was maintained at 250 °C, and the oven temperature was ramped from 180 °C to 240 °C at 10 °C/min, with a final 10-minute hold. Electron ionization (70 eV) was used to generate ions, and total ion chromatograms were obtained for the derivatization products across the standard curve.

Immunohistochemistry

Fixed brain hemispheres were rinsed in 0.1 M PBS and stored in fresh 0.1 M PBS for an additional 48 hours prior to paraffin embedding. Serial coronal sections spanning the olfactory bulb to the cerebellum were cut and collected at 10 µm, with every seventh section retained for staining (Usende et al., 2024). Sections were deparaffinized (60 °C, 25 min) followed by two changes of xylene, then rehydrated through a descending ethanol series to distilled water. Antigen retrieval was performed in 10 mM citrate buffer (pH 6.0) for 25 minutes, followed by peroxidase quenching in hydrogen peroxide for 10 minutes and protein blocking (Abcam ab236469) for 10 minutes at room temperature in a humidity chamber. Sections were incubated overnight at 4 °C with polyclonal rabbit primary antibodies against GFAP (Abcam ab7260), IBA1 (Abcam ab153696), and parvalbumin (Abcam ab11427), each used according to the manufacturer's recommended dilution (1:1000 for ab7260, 1:1000 for ab153696 and 1 µg/mL for ab11427 respectively). Antibody binding was visualized using a rabbit-specific HRP/DAB micro-polymer detection kit (Abcam ab236469) per the manufacturer's protocol. Sections were counterstained with Mayer's modified haematoxylin (Abcam ab220365), dehydrated through an ascending ethanol series, cleared in xylene, and coverslipped with Permount. Images were captured using an Olympus CX31 light microscope connected to a digital camera and computer workstation (HP Envy).

Quantitative image analysis

Regional cell counts and soma area measurements for GFAP+, IBA1+, and parvalbumin-positive cells were performed by two experimenters blinded to experimental group, following previously described methods (Usende et al., 2024, 2022), using a Leica DM300 bright-field microscope connected to an Excelis HDS (1080p) camera and ImageJ software (NIH, Bethesda, MD, USA), at ×10 (cell counts) and ×20 (soma area) magnification. Analysis was performed on five evenly spaced sections per brain region from four brains per group, with sections sampled at 10 µm intervals across the rostro-caudal extent from the olfactory bulb to the cerebellum. Regions of interest were assessed using an optical fractionator approach (West, 1993) with a counting frame of 100 × 100 µm, following the method of Gaykema and Goehler (2009), Gerashchenko et al. (2001), and Usende et al. (2024, 2022). An immunopositive cell was counted only when the entire labelled cell body fell within the counting frame (Usende et al., 2024; Palomba et al., 2015). For soma area measurements, the perimeter of each labelled cell body was manually traced in ImageJ, ensuring complete inclusion of the cell body; measurements from five cells per section, across five sections from four brains per group, were averaged to obtain group means ± SEM, with the number of analyzed sections used as *n* for statistical purposes.

Statistical analysis

Data were analyzed using GraphPad Prism version 9.0. All results are expressed as mean ± SEM and were compared between the control and formaldehyde-inhalation groups using an unpaired Student's *t*-test. A P-value < 0.05 was considered statistically significant.

Results

Body weight gain, brain weight and brain formaldehyde concentration

Daily body weight gain did not show an observable between-group difference during the first twenty days of exposure (Figure 1A). In the late exposure window, from days 22 to 28, body

weight gain was lower in the formaldehyde-exposed group than in the control group across the expanded time course (Figure 1B). Absolute brain weight was significantly reduced in the formaldehyde-exposed group compared with controls ($p < 0.01$; Figure 1C), and relative brain weight was also significantly reduced ($p < 0.05$; Figure 1D). Brain formaldehyde concentration was significantly higher in the formaldehyde-exposed group than in controls ($p < 0.01$; Figure 1E).

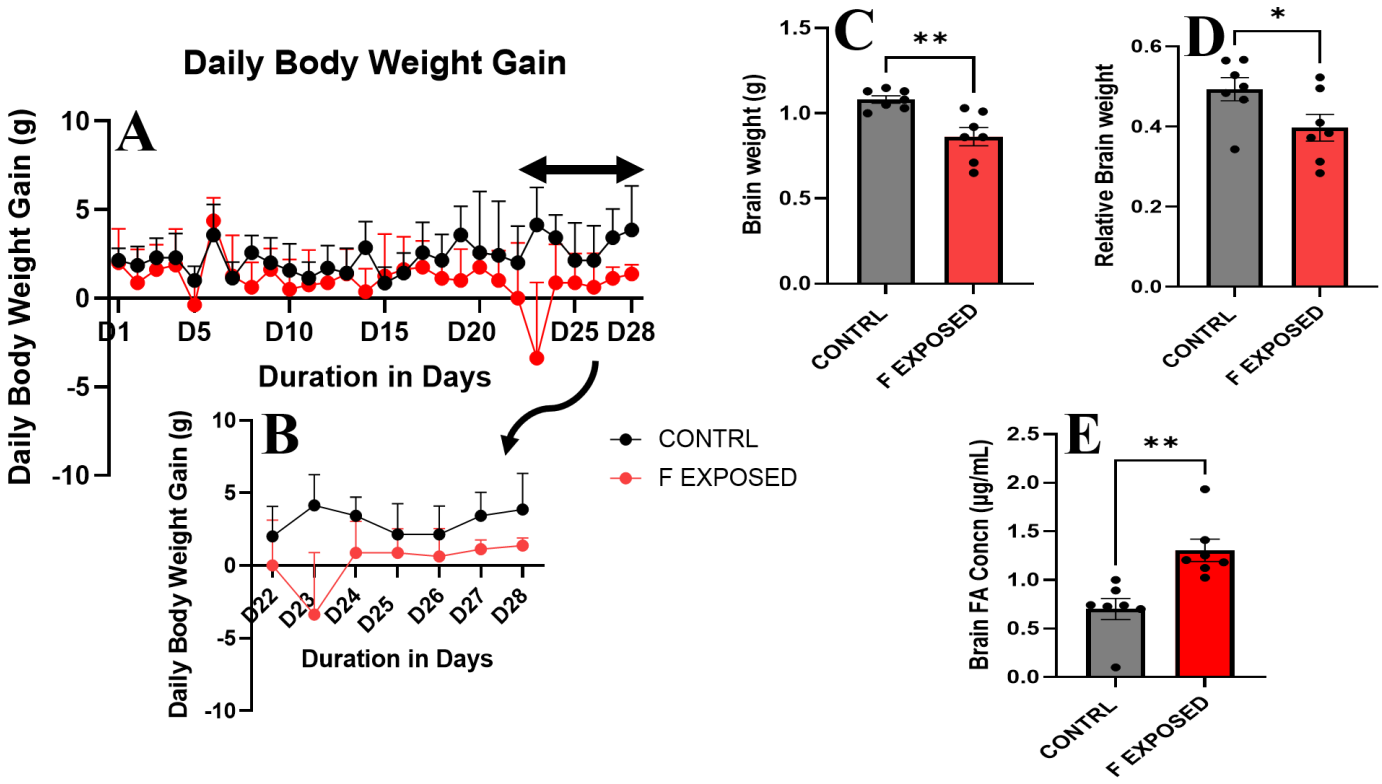


Figure 1: Body weight gain, brain weight and brain formaldehyde concentration after twenty-eight days of formaldehyde inhalation.

*Legends: Daily body weight gain from day 1 to day 28 (A); Expanded view of daily body weight gain from day 22 to day 28 (B); Absolute brain weight (C); Relative brain weight (D); Brain formaldehyde concentration (E). CTRL = Control Group; F EXPOSED = Formaldehyde-exposed Group; FA = Formaldehyde. Data are presented as mean +/SD and analysed using Student's t-test. * $p < 0.05$; ** $p < 0.01$; ns, not significant.*

Neurobehavioural performance after formaldehyde inhalation

The formaldehyde-exposed group showed a significantly shorter latency to fall in the hanging wire test than controls ($p < 0.05$; Figure 2A). In the Morris water maze, latency to find the hidden platform was significantly increased in the formaldehyde-exposed group ($p < 0.01$; Figure 2B). In the open-field test, line crossing was significantly reduced ($p < 0.001$; Figure 2C), and rearing frequency was also significantly reduced ($p < 0.05$; Figure 2D), in the formaldehyde-exposed group compared with controls. Urine drops were significantly increased in the exposed group ($p < 0.01$; Figure 2E), whereas faecal drops did not differ significantly between groups (Figure 2F).

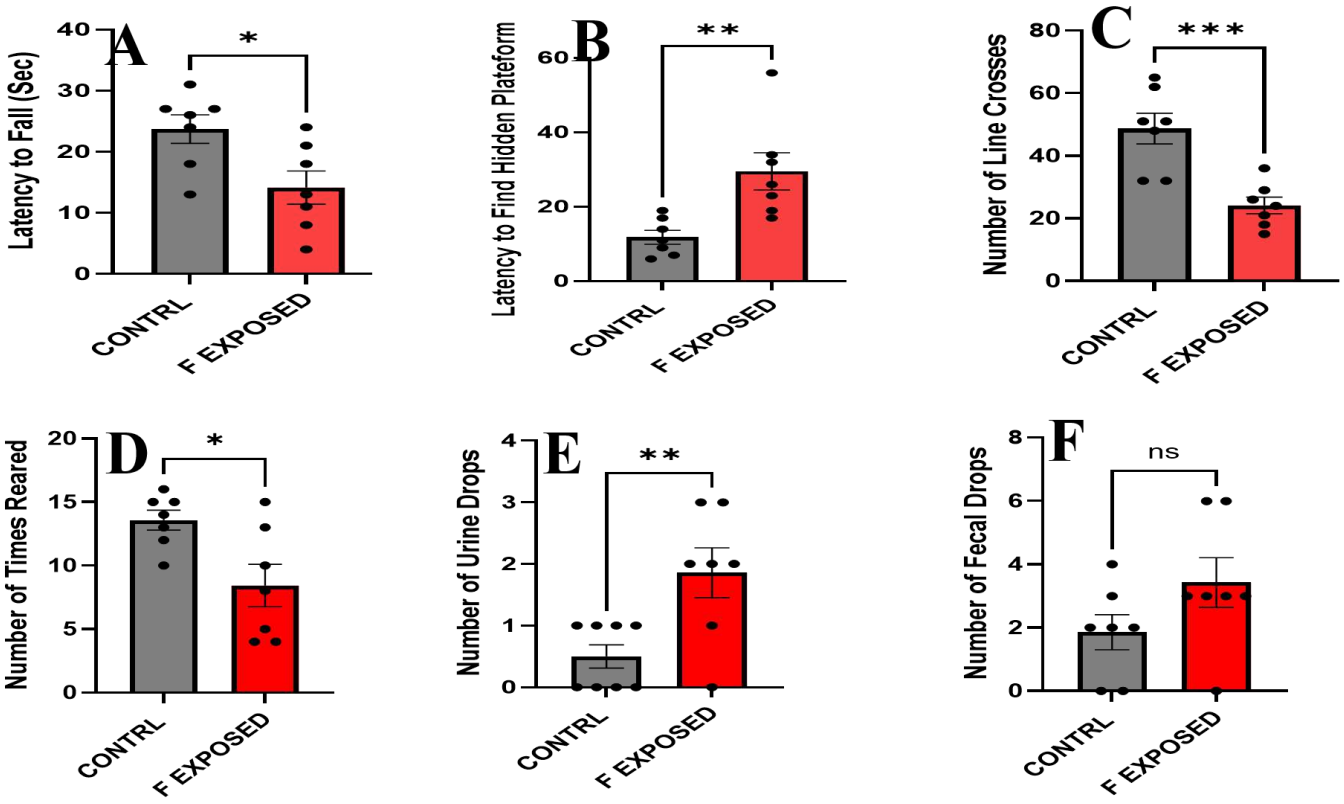


Figure 2: Behavioural test outcomes after twenty-eight days of formaldehyde inhalation.

Legends: Hanging wire test latency to fall (A); Morris water maze latency to find the hidden platform (B); Open-field line crossing (C); Open-field rearing (D); Urine drops (E); Faecal drops (F). CTRL = Control Group; F EXPOSED = Formaldehyde-exposed group. Data are

*presented as mean +/SD and analysed using Student's t-test. * $p < 0.05$; ** $p < 0.01$; *** $p < 0.001$; ns, not significant.*

Oxidative stress and antioxidant markers change following formaldehyde exposure

Malondialdehyde concentration was significantly higher in the formaldehyde-exposed group than in controls ($p < 0.05$; Figure 3A). In contrast, antioxidant indices were significantly lower in the exposed group. Catalase activity was reduced ($p < 0.05$; Figure 3B), superoxide dismutase activity showed a stronger reduction ($p < 0.01$; Figure 3C), glutathione S transferase activity was reduced ($p < 0.05$; Figure 3D), and reduced glutathione concentration was also reduced ($p < 0.05$; Figure 3E).

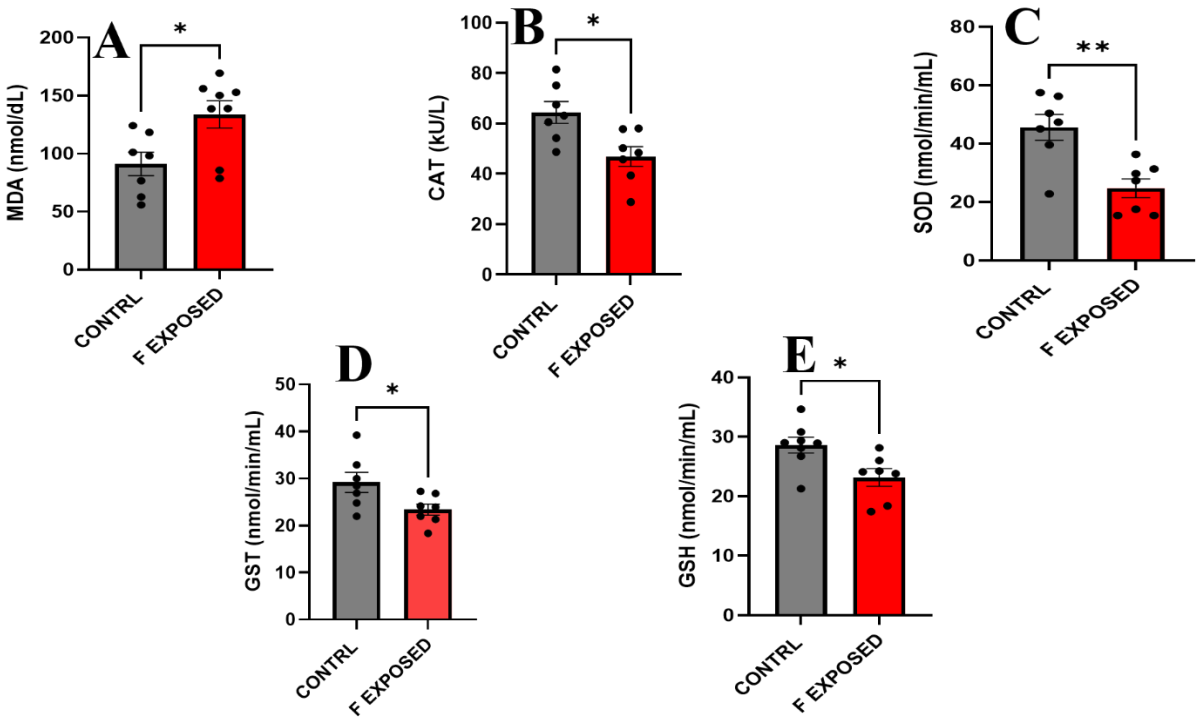


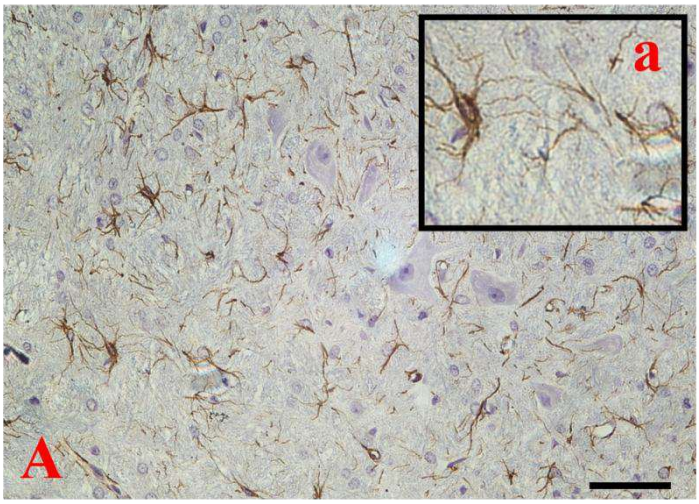
Figure 3: Oxidative stress and antioxidant markers after twenty-eight days of formaldehyde inhalation.

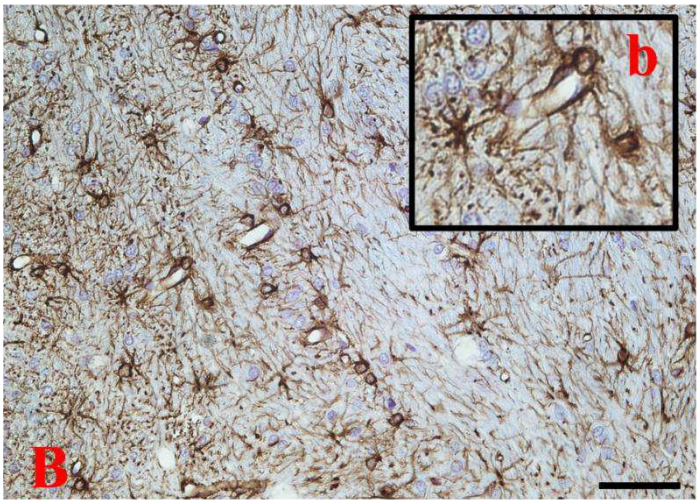
Legends: Malondialdehyde (A); Catalase (B); Superoxide dismutase (C); Glutathione S transferase (D); Reduced glutathione (E). CTRL = Control Group; F EXPOSED =

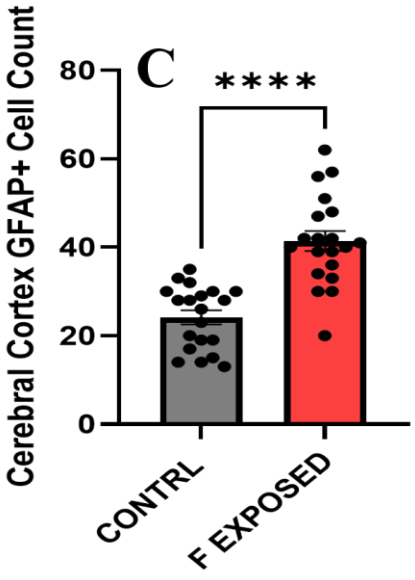
*Formaldehyde-exposed group. Data are presented as mean +/SD and analysed using Student's t-test. * $p < 0.05$; ** $p < 0.01$.*

GFAP immunoreactivity in the cerebral cortex following formaldehyde inhalation

GFAP immunostaining in the cerebral cortex showed greater astrocytic density and more prominent GFAP-positive profiles in the formaldehyde-exposed group than in controls (Figures 4A and B). Quantitative analysis showed a significant increase in GFAP-positive cell count in the exposed group ($p < 0.0001$; Figure 4C). GFAP-positive soma area was also significantly increased in the formaldehyde-exposed group compared with controls ($p < 0.01$; Figure 4D).







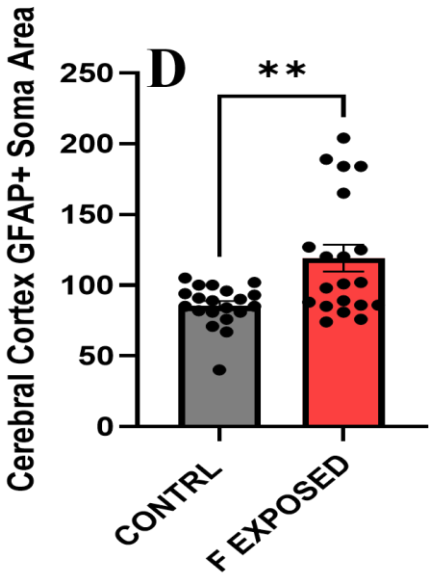


Figure 4: GFAP immunoreactivity in the cerebral cortex.

*Legends: Control cerebral cortex (A); Higher magnification insert from control cerebral cortex (a); Formaldehyde-exposed cerebral cortex (B); Higher magnification insert from formaldehyde-exposed cerebral cortex (b); Cerebral cortex GFAP positive cell count (C); Cerebral cortex GFAP positive soma area (D). GFAP = Glial Fibrillary Acidic Protein; CTRL = Control Group; F EXPOSED = Formaldehyde-exposed Group. Scale bar: 50 µm. Data are analysed using the Student t-test. ** $p < 0.01$; **** $p < 0.0001$.*

GFAP immunoreactivity in the cerebellum following formaldehyde exposure

In the cerebellum, GFAP immunostaining was more prominent in the formaldehyde-exposed group than in controls (Figures 5A and B), including the granular cell layer (Figures 5a and c) and white matter tract (Figures 5b and d). Quantification showed a significant increase in cerebellar GFAP-positive cell count in the formaldehyde-exposed group ($p < 0.0001$; Figure 5C). GFAP-positive soma area was also significantly increased after formaldehyde inhalation ($p < 0.05$; Figure 5D).

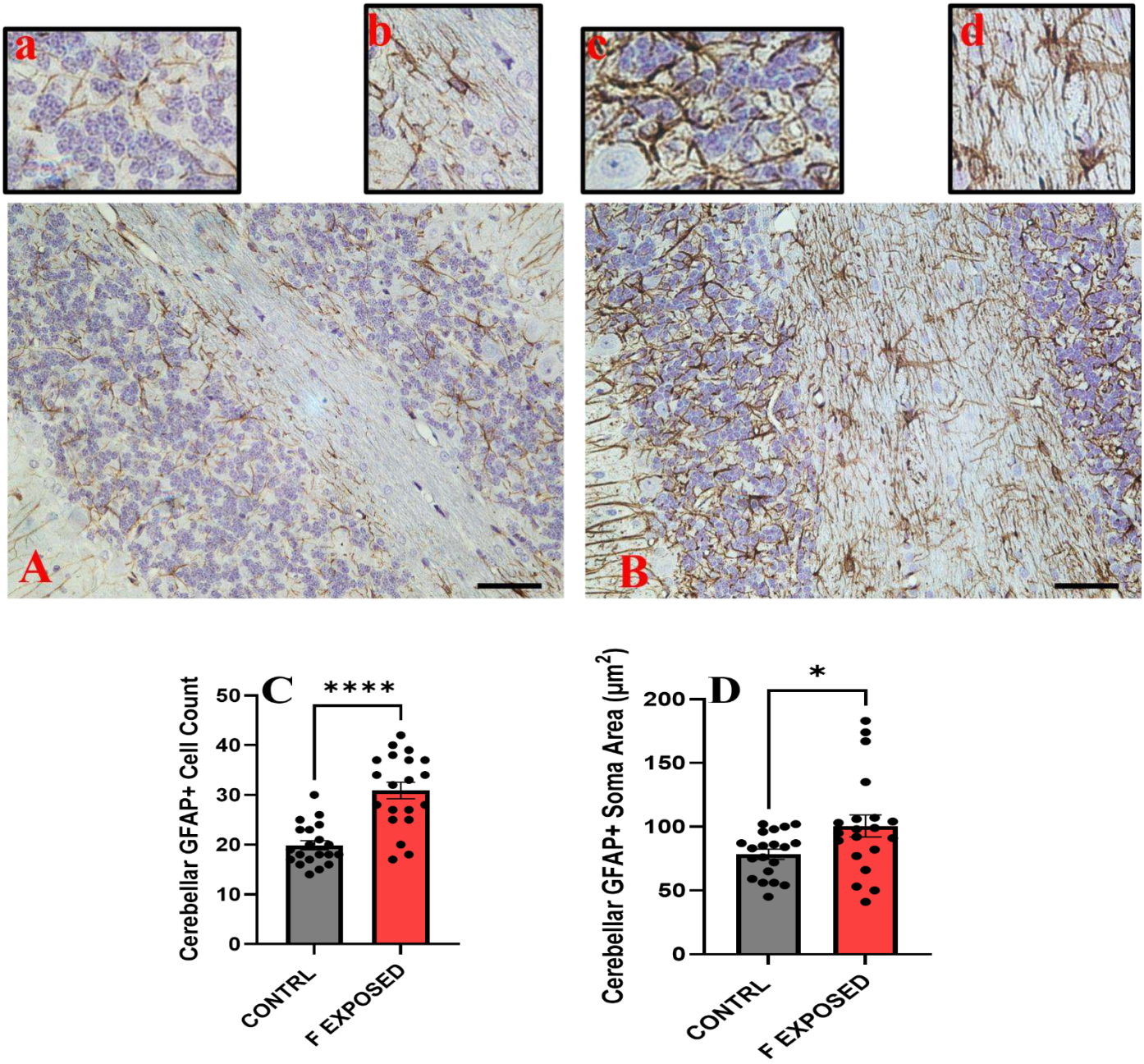
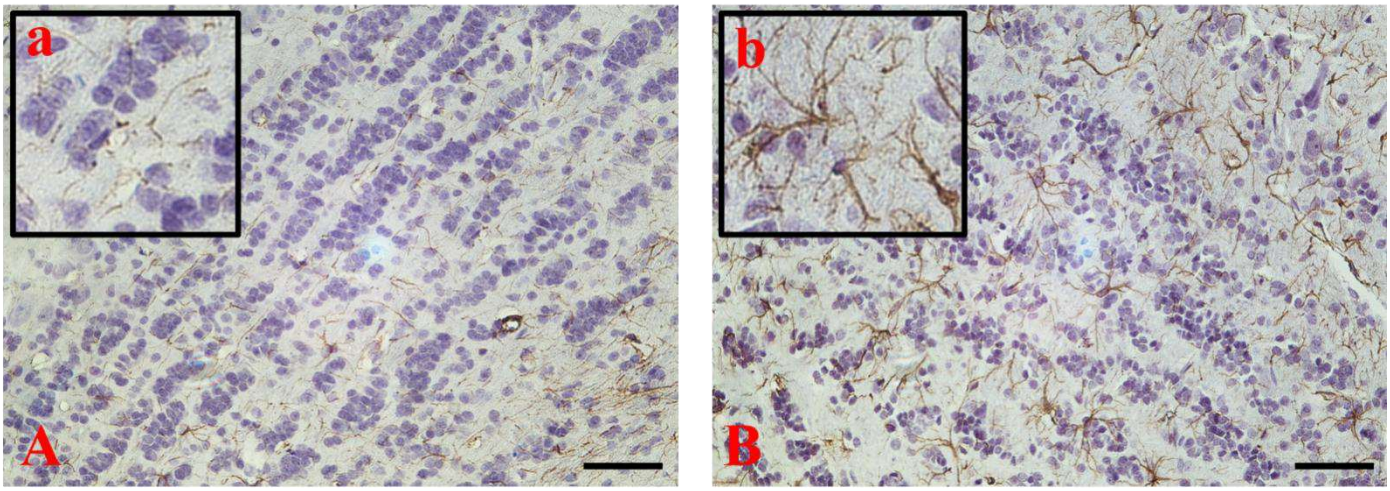


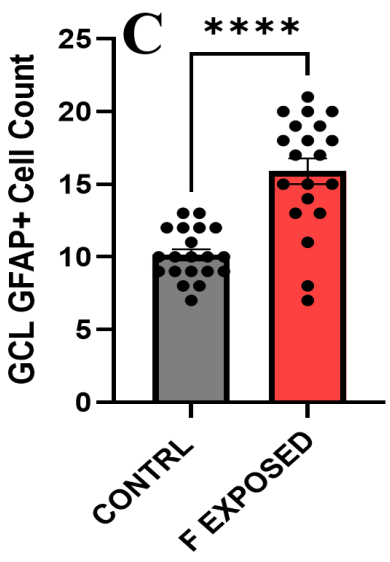
Figure 5: GFAP immunoreactivity in the cerebellum.

*Legends: Control cerebellum (A); Granular cell layer insert in control cerebellum (a); White matter tract insert in control cerebellum (b); Formaldehyde-exposed cerebellum (B); Granular cell layer insert in formaldehyde exposed cerebellum (c); White matter tract insert in formaldehyde exposed cerebellum (d); Cerebellar GFAP-positive cell count (C); Cerebellar GFAP-positive soma area (D). GFAP = Glial Fibrillary Acidic Protein; CTRL = Control Group; F EXPOSED = Formaldehyde-exposed group. Scale bar: 50 µm. Data are analysed using the Student t-test. * $p < 0.05$; **** $p < 0.0001$.*

GFAP immunoreactivity in the granule cell layer of the olfactory bulb following formaldehyde inhalation

GFAP immunostaining in the granule cell layer of the olfactory bulb was increased in the formaldehyde-exposed group compared with controls (Figures 6Aa and Bb). Quantitative analysis showed a significant increase in GFAP-positive cell count in the exposed group ($p < 0.0001$; Figure 6C). GFAP-positive soma area was also significantly increased in the formaldehyde-exposed group ($p < 0.01$; Figure 6D).





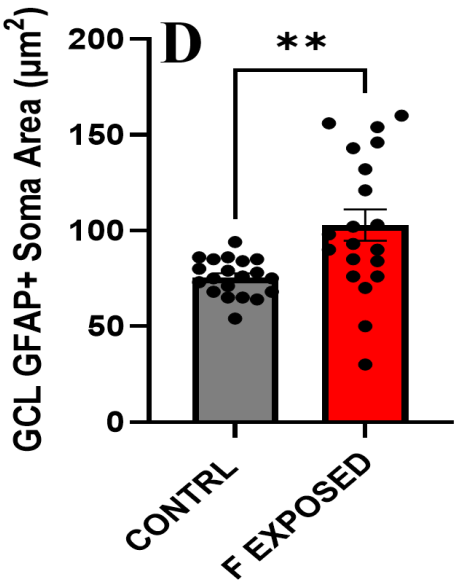


Figure 6: GFAP immunoreactivity in the granule cell layer of the olfactory bulb.

*Legends: Control granule cell layer of the olfactory bulb (A); Higher magnification insert from control tissue (a); Formaldehyde-exposed granule cell layer of the olfactory bulb (B); Higher magnification insert from formaldehyde-exposed tissue (b); Granule cell layer GFAP-positive cell count (C); Granule cell layer GFAP-positive soma area (D). GFAP = Glial Fibrillary Acidic Protein; GCL = Granule Cell Layer; OB = Olfactory Bulb; CTRL = Control Group; F EXPOSED = Formaldehyde-exposed group. Scale bar: 50 µm. Data are analysed using the Student t-test. ** $p < 0.01$; **** $p < 0.0001$.*

GFAP immunoreactivity in the external plexiform layer of the olfactory bulb following formaldehyde exposure

In the external plexiform layer of the olfactory bulb, GFAP immunoreactivity was greater in the formaldehyde-exposed group than in controls (Figures 7a and Bb). GFAP-positive cell count was significantly increased in the exposed group ($p < 0.0001$; Figure 7C). GFAP-positive soma area was also significantly higher in the formaldehyde-exposed group ($p < 0.0001$; Figure 7D).

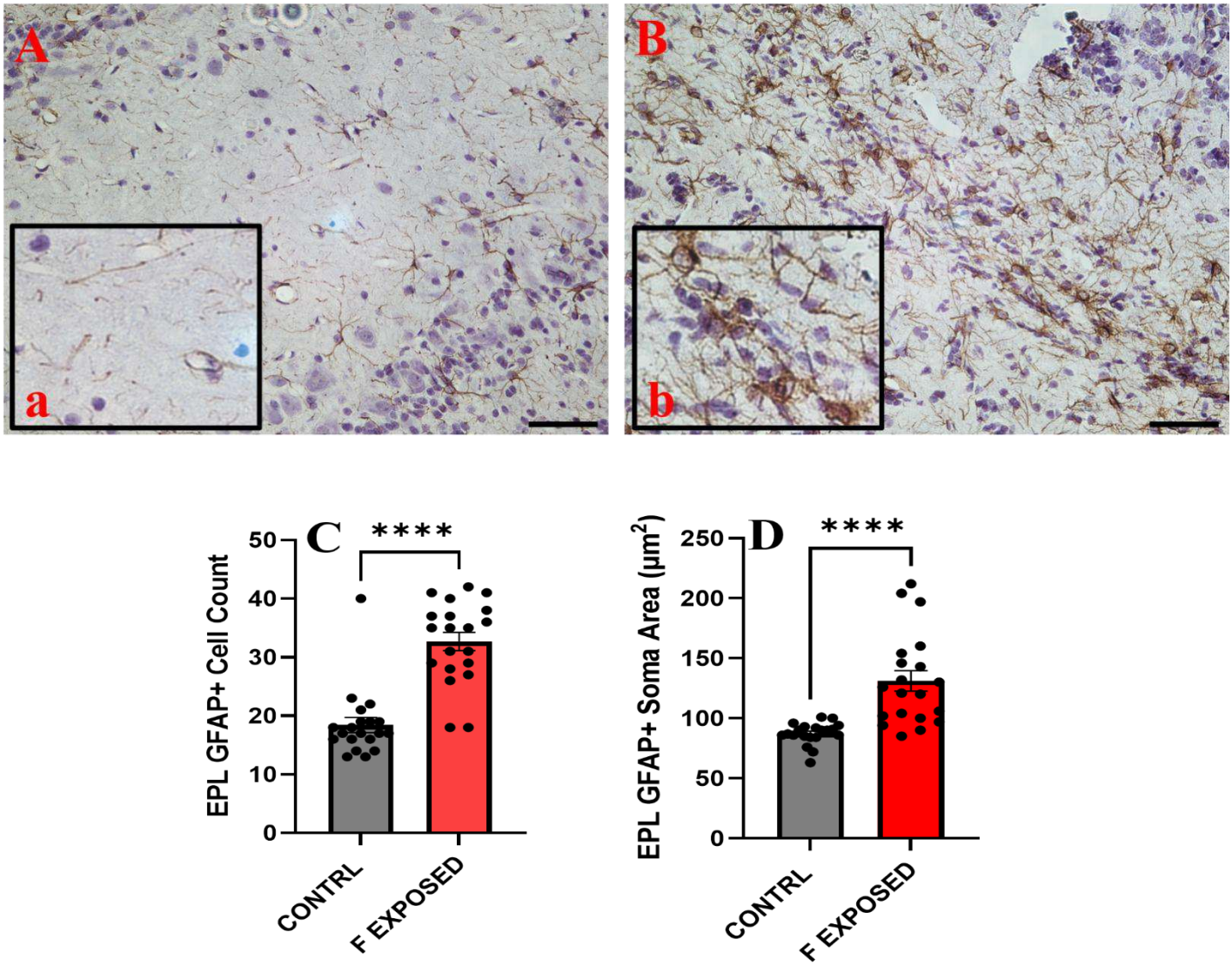


Figure 7: GFAP immunoreactivity in the external plexiform layer of the olfactory bulb.

*Legends: Control external plexiform layer of the olfactory bulb (A); Higher magnification insert from control tissue (a); Formaldehyde-exposed external plexiform layer of the olfactory bulb (B); Higher magnification insert from formaldehyde-exposed tissue (b); External plexiform layer GFAP positive cell count (C); External plexiform layer GFAP positive soma area (D). GFAP = Glial Fibrillary Acidic Protein; EPL = External Plexiform Layer; OB = Olfactory Bulb; CTRL = Control Group; F EXPOSED = Formaldehyde-exposed Group. Scale bar: 50 µm. Data are analysed using the Student t-test. **** $p < 0.0001$.*

IBA1 immunoreactivity in the hippocampus following formaldehyde inhalation

IBA1 immunostaining in the hippocampus showed increased microglial profiles in the formaldehyde-exposed group (Figures 8B and b) compared with controls (Figures 8A and a). Quantification analysis showed a significant increase in hippocampal IBA1-positive cell count in the exposed group ($p < 0.0001$; Figure 8C). Hippocampal IBA1-positive soma area was also significantly increased in the formaldehyde-exposed group ($p < 0.0001$; Figure 8D).

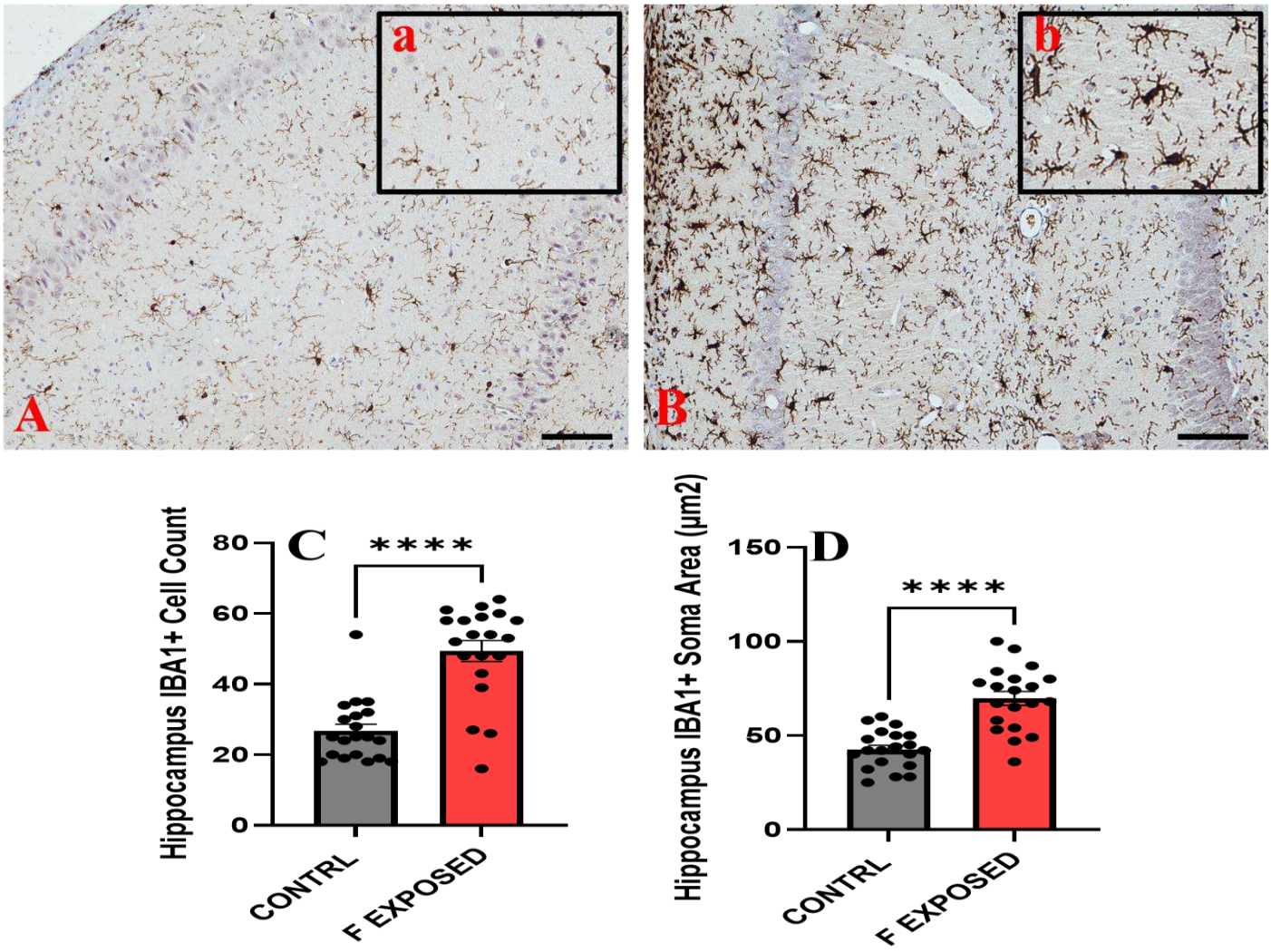


Figure 8: IBA1 immunoreactivity in the hippocampus.

Legends: Control hippocampus (A); Higher magnification insert from control hippocampus (a); Formaldehyde exposed hippocampus (B); Higher magnification insert from formaldehyde

*exposed hippocampus (b); Hippocampal IBA1 positive cell count (C); Hippocampal IBA1 positive soma area (D). IBA1 = Ionized Calcium Binding Adaptor Molecule 1; CTRL = Control Group; F EXPOSED = Formaldehyde exposed group. Scale bar: 50 µm. Data are analysed using Student t test. **** $p < 0.0001$.*

IBA1 immunoreactivity in the dentate gyrus following formaldehyde exposure

In the dentate gyrus, IBA1 immunoreactivity was increased in the formaldehyde-exposed group (Figures 9B and b) relative to controls (Figures 9A and a). IBA1 positive cell count was significantly higher in the exposed group ($p < 0.001$; Figure 9C). IBA1-positive soma area was also significantly increased in the formaldehyde-exposed group ($p < 0.001$; Figure 9D).

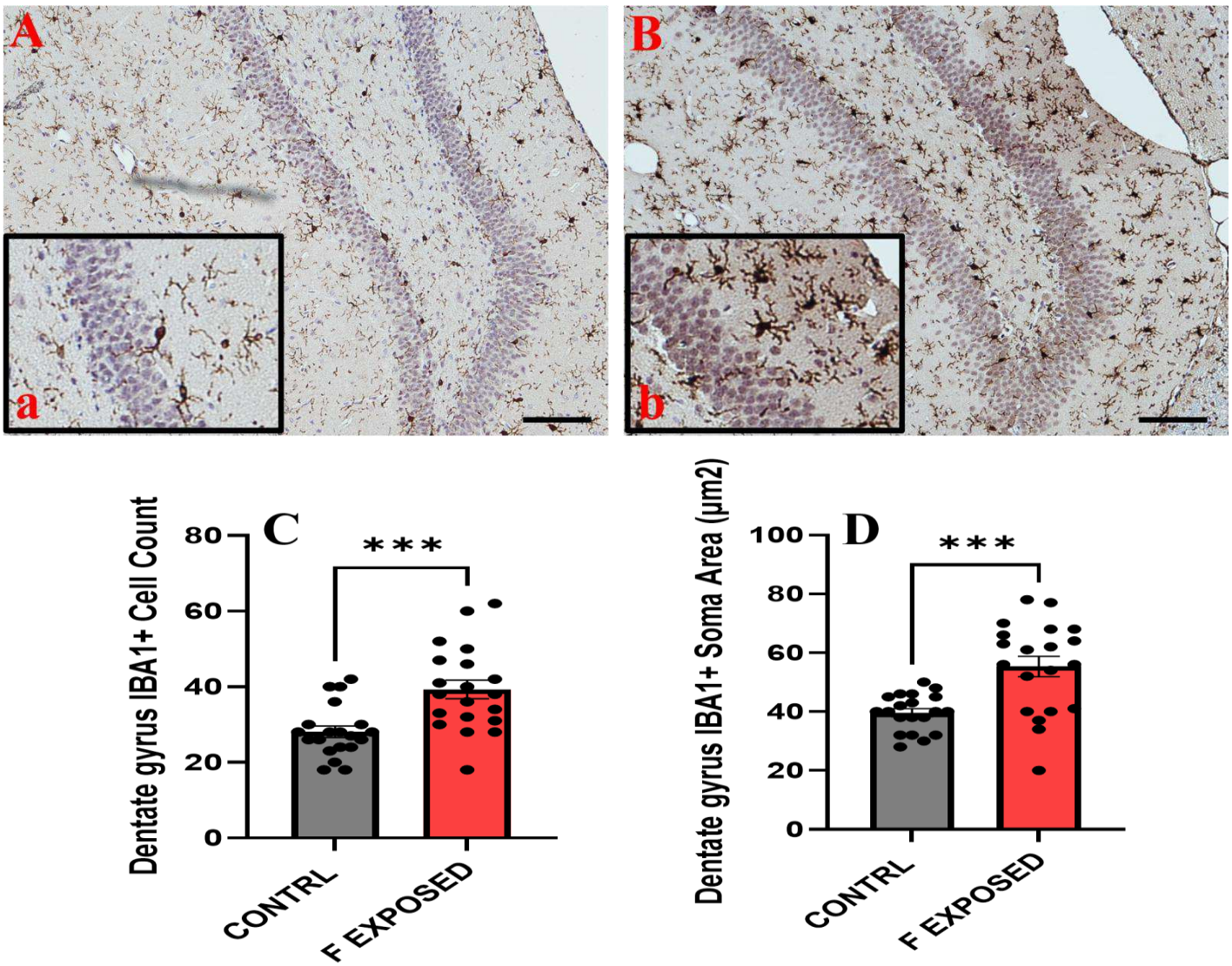


Figure 9: IBA1 immunoreactivity in the dentate gyrus.

*Legends: Control dentate gyrus (A); Higher magnification insert from control tissue (a); Formaldehyde exposed dentate gyrus (B); Higher magnification insert from formaldehyde exposed tissue (b); Dentate gyrus IBA1 positive cell count (C); Dentate gyrus IBA1 positive soma area (D). IBA1 = Ionized Calcium Binding Adaptor Molecule 1; CTRL = Control Group; F EXPOSED = Formaldehyde exposed Group. Scale bar: 50 µm. Data are analysed using Student t test. *** $p < 0.001$.*

Figure 10. IBA1 immunoreactivity in the external plexiform layer of the olfactory bulb

IBA1 immunostaining in the external plexiform layer of the olfactory bulb was increased in the formaldehyde-exposed group (Figures 10B and b) compared with controls (Figures 10A and a). Quantitative analysis showed a significant increase in IBA1-positive cell count in the exposed group ($p < 0.0001$; Figure 10C). IBA1-positive soma area was also significantly increased in the formaldehyde-exposed group ($p < 0.0001$; Figure 10D).

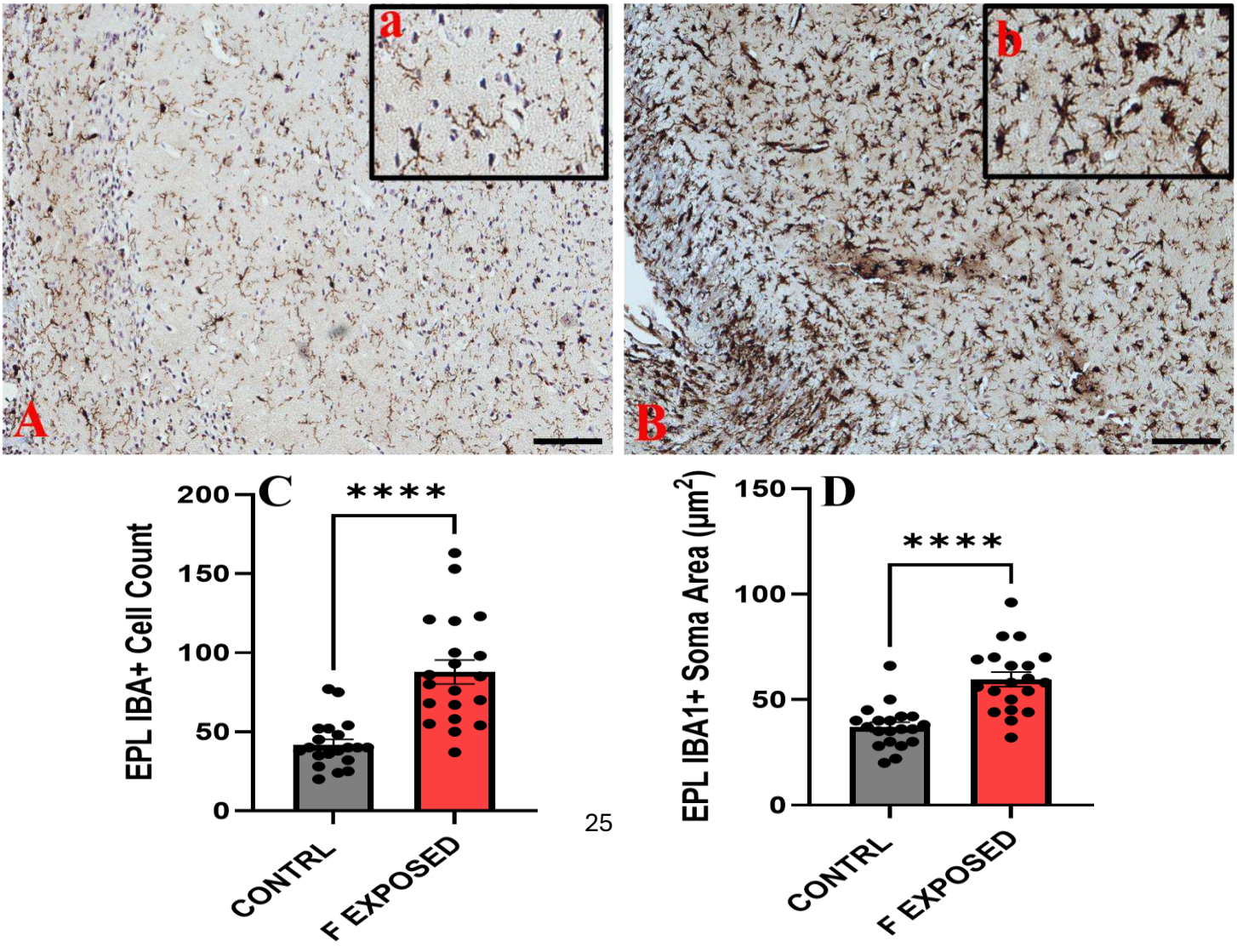


Figure 10: IBA1 immunoreactivity in the external plexiform layer of the olfactory bulb.

*Legends: Control external plexiform layer of the olfactory bulb (A); Higher magnification insert from control tissue (a); Formaldehyde exposed external plexiform layer of the olfactory bulb (B); Higher magnification insert from formaldehyde exposed tissue (b); External plexiform layer IBA1 positive cell count (C); External plexiform layer IBA1 positive soma area (D). IBA1 = Ionized Calcium Binding Adaptor Molecule 1; EPL = External Plexiform Layer; OB = Olfactory Bulb; CTRL = Control Group; F EXPOSED = Formaldehyde-exposed group. Scale bar: 50 µm. Data are analysed using the Student t-test. **** $p < 0.0001$.*

IBA1 immunoreactivity in the mitral and inner plexiform layers of the olfactory bulb

In the mitral and inner plexiform layers of the olfactory bulb, IBA1 immunoreactivity was higher in the mitral cell layer (Figure 11c) and inner plexiform layer (Figure 11d) of the formaldehyde-exposed group than in control's (Figure 11A), mitral cell (Figure 11a) and inner plexiform (Figure 11b) layers. IBA1 positive cell count was significantly increased in the exposed group ($p < 0.0001$; Figure 11C). IBA1-positive soma area was also significantly increased in the formaldehyde-exposed group, although at a lower statistical threshold than the cell count ($p < 0.01$; Figure 11D).

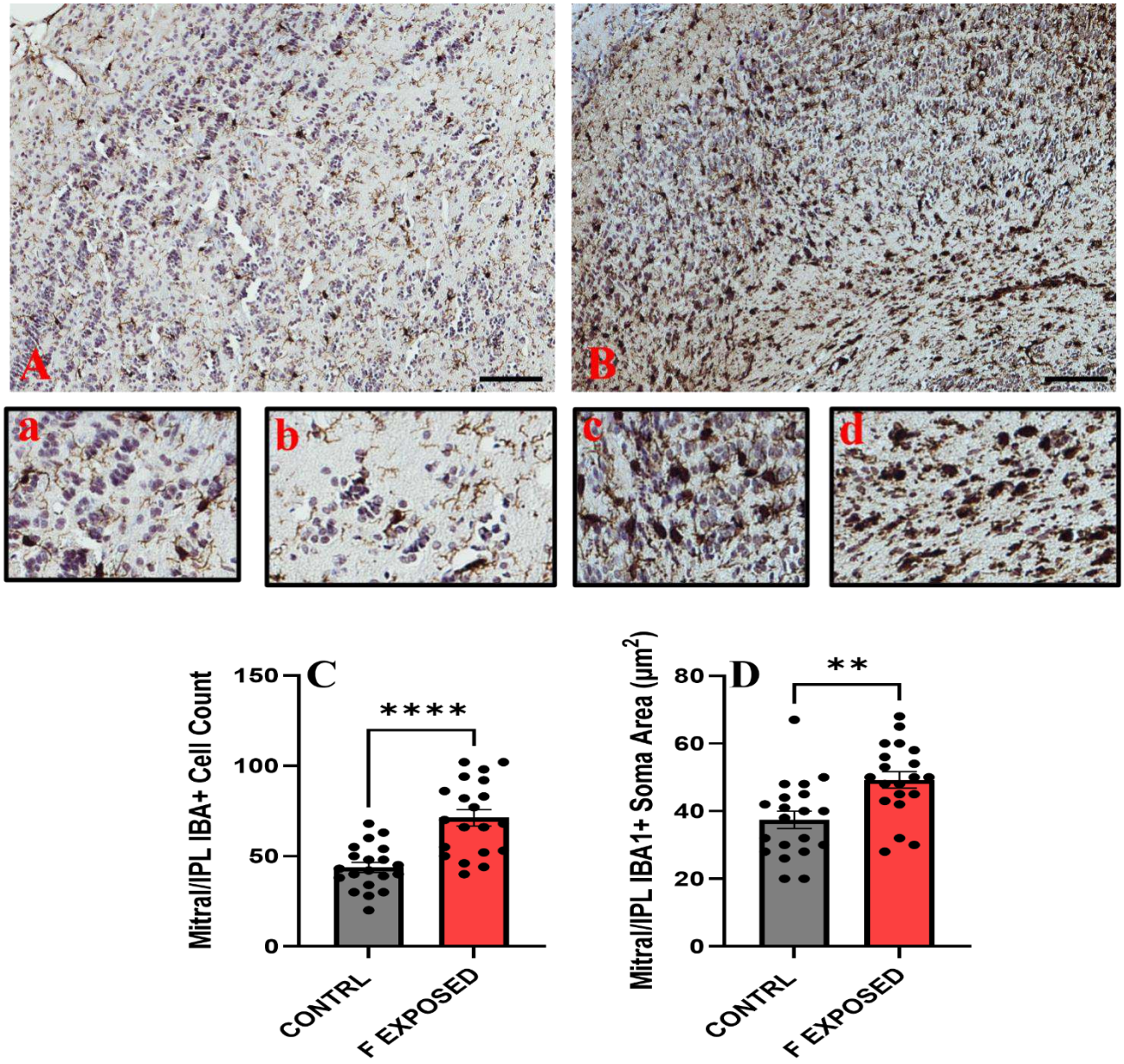


Figure 11: IBA1 immunoreactivity in the mitral and inner plexiform layers of the olfactory bulb. *Legends: A, control olfactory bulb; a, mitral cell layer insert in control tissue; b, inner plexiform layer insert in control tissue; B, formaldehyde exposed olfactory bulb; c, mitral cell layer insert in formaldehyde exposed tissue; d, inner plexiform layer insert in formaldehyde exposed tissue; C, mitral and inner plexiform layer IBA1 positive cell count; D, mitral and inner plexiform layer IBA1 positive soma area. IBA1, ionized calcium binding adaptor molecule 1; IPL, inner plexiform layer; OB, olfactory bulb; CTRL, control group; F EXPOSED, formaldehyde-exposed group. Scale bar: 50 µm. Data are analysed using the Student t-test. ** $p < 0.01$; **** $p < 0.0001$.*

Parvalbumin immunoreactivity in the cerebellum following formaldehyde inhalation

Immunohistochemical analysis revealed distinct differences in the cerebellar parvalbumin (PV) interneurons between control and formaldehyde-exposed rats (Figure 12). In the control group (A–C), PV-positive Purkinje neurons appeared normal, well distributed, and exhibited fine dendritic arborization within the Purkinje cell layer. In contrast, the formaldehyde-inhaled group (D–I) showed severe neuronal loss, shrinkage of Purkinje cell somata, and marked reduction in dendritic arborization. Quantitative stereological assessment further confirmed these observations. Bar graphs (Figure 12J–K) demonstrated a significantly reduced number of PV-positive neurons and smaller soma areas in the formaldehyde-exposed group compared to controls (****$p < 0.0001$, Student's t-test). Scale bars: 50 μm in A and G; 40 μm in B, C, E, and F.

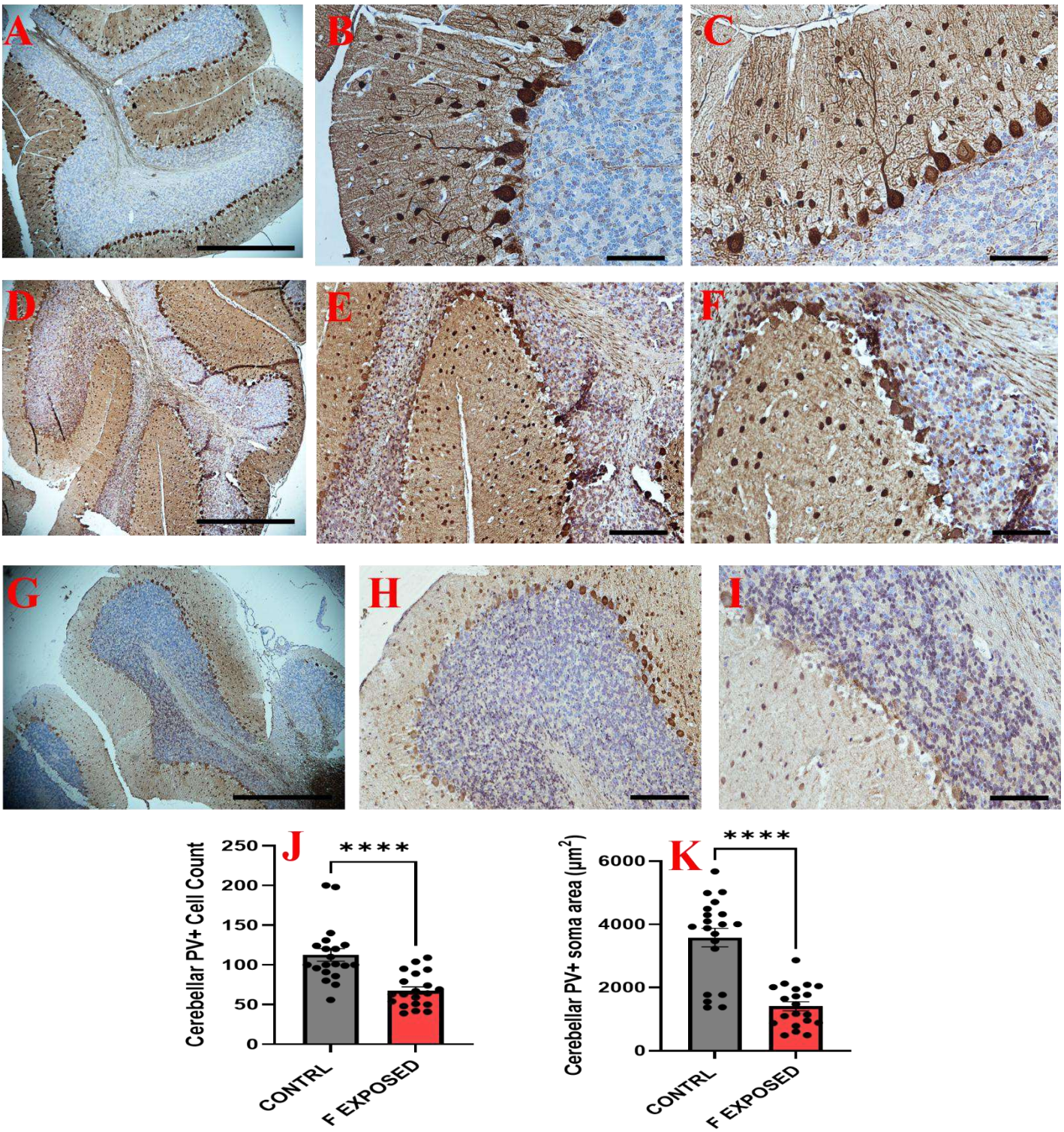


Figure 12: Parvalbumin immunoreactivity in the cerebellum.

*Legends: A to C, control cerebellar sections; D to I, formaldehyde-exposed cerebellar sections; J, cerebellar PV-positive cell count; K, cerebellar PV-positive soma area. PV, parvalbumin; CTRL, control group; F EXPOSED, formaldehyde-exposed group. Scale bars: 50 µm in A and G; 40 µm in B, C, E and F. Data are analysed using Student's t-test. **** $p < 0.0001$.*

Parvalbumin immunoreactivity in the CA1 region of the hippocampus following formaldehyde exposure

Immunoreactivity of fast-spiking inhibitory parvalbumin (PV) interneurons in the CA1 region of the hippocampus revealed clear differences between control and formaldehyde-exposed rats (Figure 13). In the control group (A), PV-positive neurons appeared normal in number and size. In contrast, the formaldehyde-inhaled group (B) showed a marked reduction in both the number and soma size of PV-positive cells. Scale bar: 50 µm. Quantitative stereological analysis supported these observations. Bar graphs (Figure 13C–D) demonstrated a significant reduction in PV-positive neuron counts and soma area in the formaldehyde-exposed group compared to controls (***p < 0.001, ****p < 0.0001, Student's t-test).

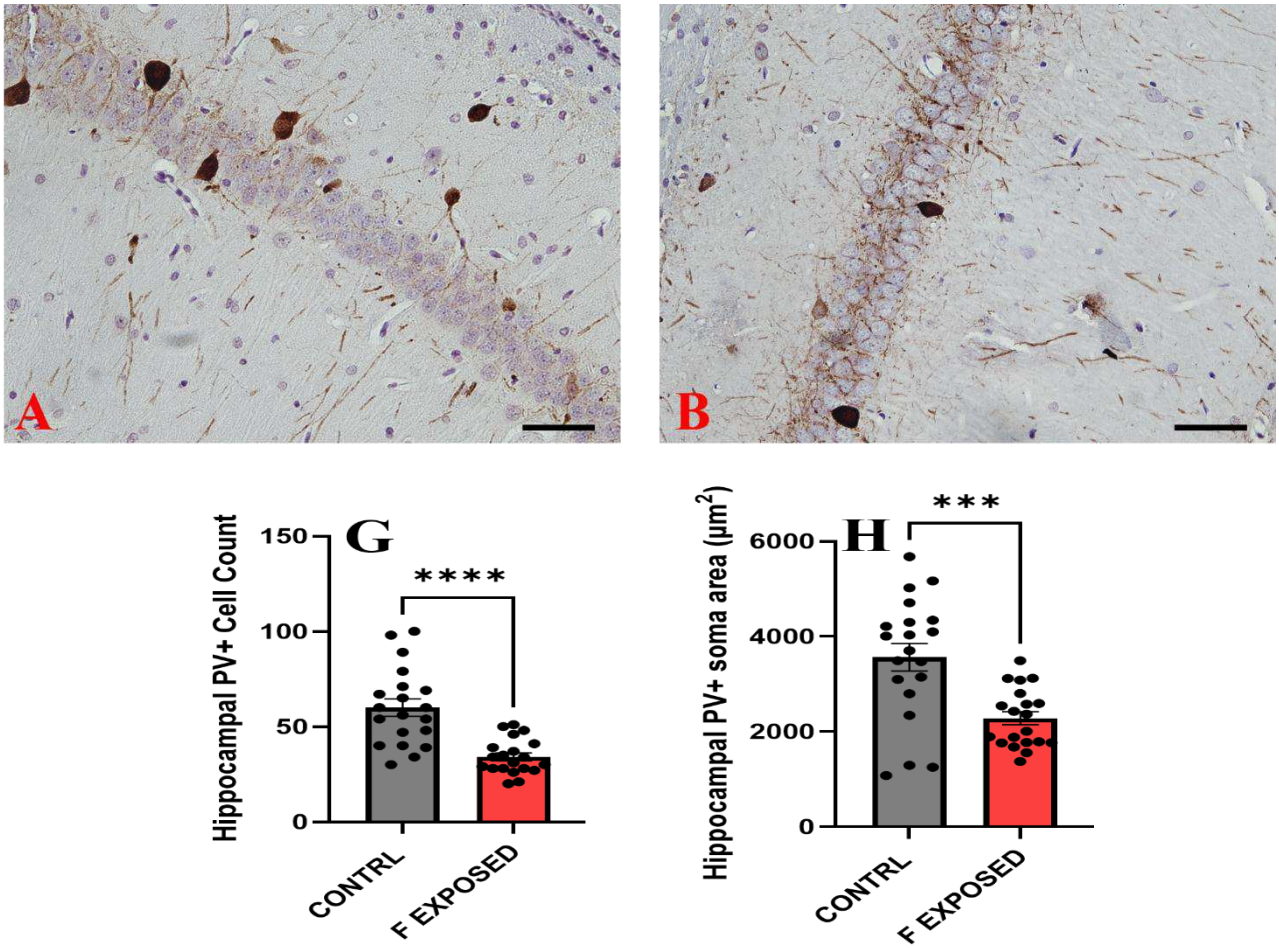
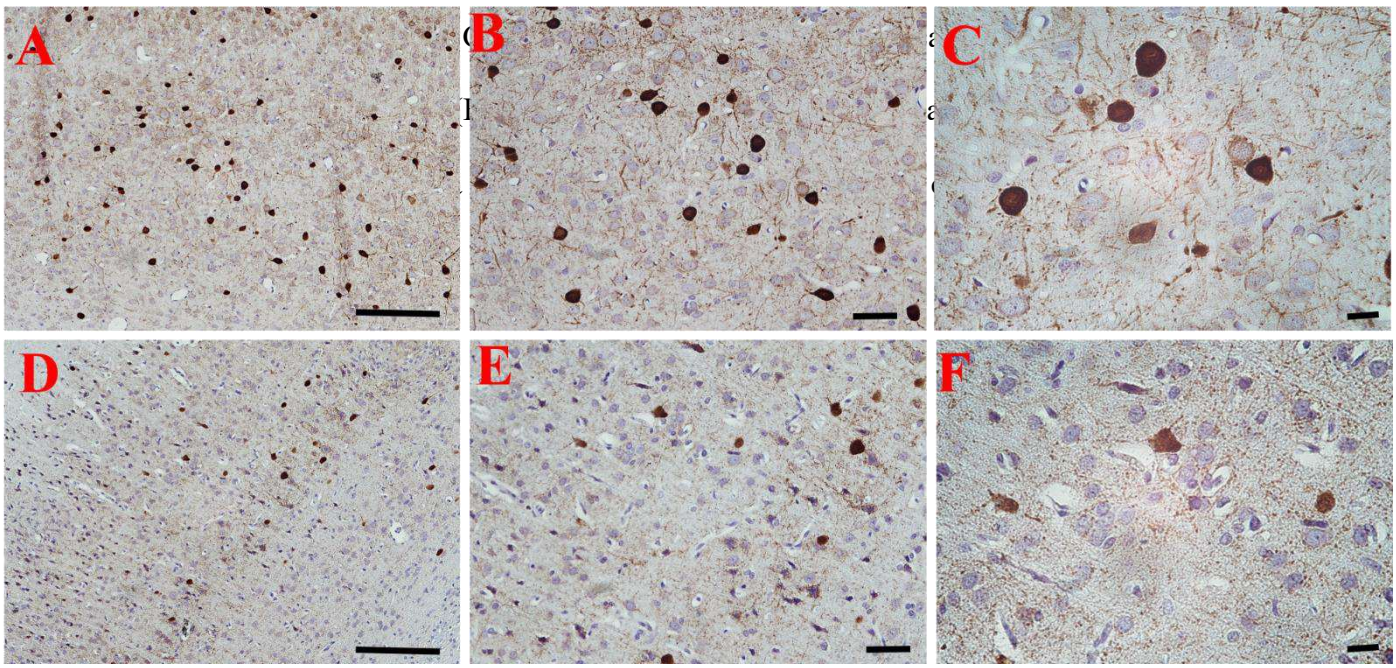


Figure 13. Parvalbumin immunoreactivity in the CA1 region of the hippocampus.

*Legends: A, control hippocampal CA1 region; B, formaldehyde-exposed hippocampal CA1 region; G, hippocampal PV positive cell count; H, hippocampal PV positive soma area. PV, parvalbumin; CTRL, control group; F EXPOSED, formaldehyde-exposed group. Scale bar: 50 µm. Data are analysed using the Student t-test. *** $p < 0.001$; **** $p < 0.0001$.*

Parvalbumin immunoreactivity in the cerebral cortex following formaldehyde exposure

Immunoreactivity of fast-spiking inhibitory parvalbumin (PV) interneurons in the cerebral cortex revealed marked differences between control and formaldehyde-exposed rats (Figure 14). In the control group (A–C), PV-positive neurons appeared normal in number, soma size, and dendritic arborization. In contrast, the formaldehyde-inhaled group (D–F) exhibited reduced neuronal counts, smaller somata, and diminished dendritic arborization. Scale bars: 50



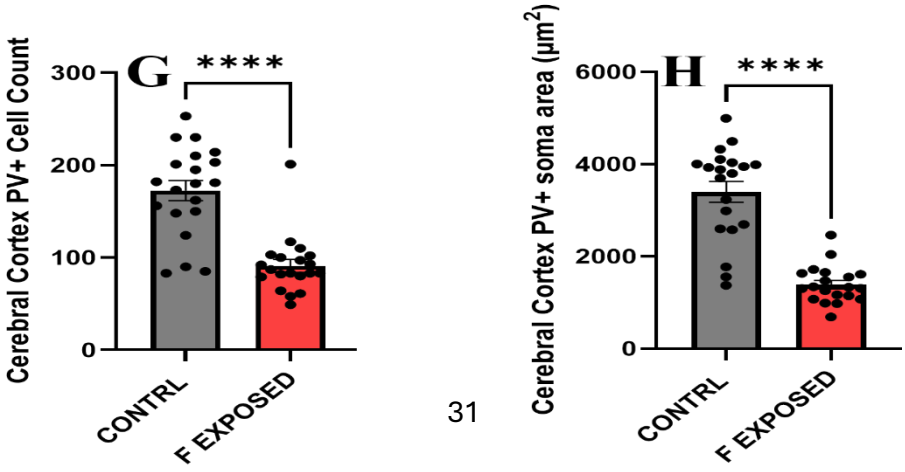


Figure 14. Parvalbumin immunoreactivity in the cerebral cortex.

*Legends: A to C, control cerebral cortex; D to F, formaldehyde-exposed cerebral cortex; G, cerebral cortex PV-positive soma area; H, cerebral cortex PV-positive cell count. PV, parvalbumin; CTRL, control group; F EXPOSED, formaldehyde-exposed group. Scale bars: 50 µm in A and G; 40 µm in B, C, E and F. Data are analysed using Student's t-test. **** $p < 0.0001$.*

Discussion

This study demonstrates that 28-day inhalational exposure to formaldehyde produces a coordinated pattern of systemic, behavioural, biochemical, and cellular disruption in the rat brain: reduced body and brain weight, impaired motor and cognitive performance, elevated oxidative stress with depleted antioxidant reserve, and a marked, region-dependent loss of parvalbumin-expressing, fast-spiking GABAergic interneurons accompanied by pronounced astrocytic and microglial activation. Taken together, these findings extend the existing formaldehyde neurotoxicity literature in a direction that has not, to our knowledge, been previously resolved at the cellular level: the differential regional vulnerability of a specific, functionally defined interneuron population under a chronic, occupationally relevant inhalation paradigm.

The reductions in catalase, superoxide dismutase, glutathione-S-transferase, and reduced glutathione, alongside elevated malondialdehyde, indicate that formaldehyde inhalation overwhelmed the brain's endogenous antioxidant capacity well before the 28-day endpoint. This redox imbalance offers a plausible explanation for why parvalbumin interneurons in particular, rather than neurons generally, bore the brunt of the damage observed on immunohistochemistry. Fast-spiking interneurons sustain unusually high rates of oxidative phosphorylation, supported by an elevated mitochondrial and cytochrome c oxidase content, to sustain their rapid, sustained firing, and this metabolic profile appears to leave them with

comparatively little buffering capacity against exogenous oxidative insult (Kann & Kovács, 2007; Kann, 2016). Developmental and metabolic-stress models converge on the same conclusion: glutathione depletion selectively compromises parvalbumin interneuron structure and connectivity while sparing neighbouring neuronal populations to a much greater degree, and this vulnerability can be reproduced pharmacologically through NADPH-oxidase-driven superoxide generation (Cabungcal et al., 2006; Behrens et al., 2007). Perineuronal nets, which mature around parvalbumin interneurons and normally confer partial protection against oxidative stress, may not have been sufficient to buffer the magnitude or duration of the insult modelled here (Steullet et al., 2010; Cabungcal et al., 2013). Our data are consistent with this pattern operating under a toxicological, rather than a developmental or psychiatric, insult.

A second, complementary mechanism may run in parallel with oxidative stress rather than in place of it. Formaldehyde is a well-characterized cross-linking agent: it reacts with the amine and thiol groups of proteins to form methylol adducts that dehydrate into reactive Schiff bases, which then form stable methylene bridges with neighbouring nucleophilic residues on adjacent proteins or DNA (Tretyakova et al., 2015). Parvalbumin itself is a small, cysteine- and lysine-rich calcium-buffering protein, and calcium-buffering capacity is central to how these interneurons tolerate their own high firing rates without excitotoxic self-damage. Because the brain also generates formaldehyde endogenously as a by-product of normal one-carbon and amine metabolism, and because this endogenous pool already rises with age, an exogenous inhalational load may push cumulative formaldehyde exposure in fast-spiking interneurons past a threshold that the cell's calcium-buffering and antioxidant systems can no longer compensate for (Tulpule & Dringen, 2013; Tong et al., 2013). It is plausible, though we did not test this directly, that direct formaldehyde adduction of parvalbumin or of the calcium-handling machinery around it compounds the oxidative burden already described, producing a two-hit

vulnerability specific to this interneuron class. We raise this as a hypothesis for future biochemical work, not as a claim our current data can support on their own.

The regional pattern of vulnerability we observed maps sensibly onto the recorded behavioural deficits. Loss of Purkinje-layer parvalbumin interneurons in the cerebellum accompanies the reduced latency to fall on the forelimb grip test, consistent with disrupted cerebellar coordination of fine motor output. Loss in the CA1 hippocampal region accompanies impaired performance in the Morris water maze, consistent with the established role of parvalbumin-mediated gamma-band synchrony in hippocampal-dependent spatial learning and memory (Sohal et al., 2009; Cardin et al., 2009). Cortical interneuron loss, together with the marked reduction in open-field line crossing and rearing, is consistent with disrupted cortical inhibitory tone contributing to the anxiety-like phenotype observed. We do not claim direct causal evidence for these links from a correlational study, but the anatomical and functional correspondence across all domains tested strengthens the overall coherence of the model.

The glial response we documented, including increased GFAP-positive astrocyte number and hypertrophy, and increased IBA1-positive microglial number with amoeboid morphology in several regions, most likely represents both a consequence of, and a further contributor to, the interneuron loss described above. Reactive astrocytes and activated microglia are recruited by oxidative and cellular damage, but they themselves release additional reactive oxygen species, nitric oxide, and pro-inflammatory cytokines (Sofroniew & Vinters, 2010; Kettenmann et al., 2011), and microglia can further convert astrocytes into the neurotoxic A1 reactive phenotype that actively promotes neuronal death rather than merely reflecting it (Liddelow et al., 2017). This is expected to compound the redox burden already imposed by formaldehyde, suggesting a self-reinforcing cycle, rather than a single insult-and-response event, over the 28-day exposure window.

Several recent studies have examined formaldehyde inhalation in Wistar rats and have reported neurobiological alterations associated with chronic exposure, including hippocampal oxidative stress, inflammatory responses, and behavioural impairments. Formaldehyde inhalation has been shown to increase oxidative damage, disrupt antioxidant defence systems, and alter hippocampal synaptic function, particularly in experimental models involving prolonged exposure (Liu et al., 2010; Zararsiz et al., 2007; Zhang et al., 2025; Tang et al., 2013). Other studies have investigated formaldehyde toxicity in combination with additional physiological stressors or therapeutic interventions, demonstrating that exposure may amplify inflammatory signalling, oxidative imbalance, and neuronal injury markers under those conditions (Songur et al., 2010). These findings establish that chronic formaldehyde exposure is neurotoxic in a broad sense; however, previous studies have largely focused on biochemical alterations, behavioural outcomes, or general markers of neural injury rather than identifying selectively vulnerable neuronal subpopulations.

Parvalbumin-expressing interneurons constitute a biologically plausible population for selective vulnerability because of their high metabolic demand, extensive mitochondrial activity, and sensitivity to oxidative disturbances (Kann & Kovács, 2007; Hu et al., 2014; Steullet et al., 2017). Nevertheless, whether chronic inhalational formaldehyde exposure preferentially affects these interneurons, and whether such effects differ across anatomically distinct regions, remains unreported or unclear. The present study isolates formaldehyde inhalation as the primary experimental variable without a comorbid stressor or pharmacological intervention and applies region-specific stereological quantification of parvalbumin-expressing interneurons across the cerebellum, hippocampus, cerebral cortex, and olfactory bulb. To our knowledge, this is the first investigation to characterize regional parvalbumin interneuron alterations alongside astrocytic and microglial responses following a chronic inhalational

formaldehyde exposure paradigm, providing a cellular-resolution perspective beyond the gross biochemical changes previously reported.

Public health and occupational implications

Formalin remains the fixative of choice in the overwhelming majority of gross anatomy laboratories, and personnel, students, technicians, and academic staff alike are exposed to its vapour repeatedly, often for years, under ventilation conditions that frequently exceed recommended occupational ceiling limits and the Group 1 carcinogen classification already assigned to formaldehyde (IARC, 2006). Engineering interventions such as local exhaust ventilation and redesigned dissection tables have been shown to substantially reduce personal exposure levels in comparable settings (Akbar-Khanzadeh et al., 1994; Coleman, 1995; Keil et al., 2001), yet such controls remain unevenly implemented, particularly in resource-limited anatomy departments. If even a fraction of the cellular vulnerability demonstrated here in rats translates to long-term human exposure, it raises a legitimate concern that repeated, sub-acute formaldehyde inhalation over a career in anatomical sciences could contribute to cumulative, subclinical deficits in motor coordination, memory, or affect regulation among those most heavily exposed. This is not a claim we can make directly from an animal model, but it is precisely the kind of translational concern that justifies studying formaldehyde inhalation through an anatomically and behaviorally resolved lens rather than treating it purely as a chemical safety or respiratory issue. Practical implications include reinforcing ventilation and personal protective standards in dissection halls, particularly in low- and middle-income settings where local exhaust systems remain the exception rather than the norm, evaluating formaldehyde-sparing or formaldehyde-free embalming alternatives where feasible, and considering periodic biomonitoring for staff with prolonged occupational exposure.

Limitations

Several limitations should temper the interpretation of these findings. First, this study used a single formaldehyde concentration and a single exposure duration; a dose- and time-response design, of the kind previously used to characterize postnatal formaldehyde effects on hippocampal granule cell number (Aslan et al., 2006), would clarify whether the effects observed scale with exposure intensity and whether they are reversible after cessation of exposure. Second, only male rats were used, and sex-specific differences in formaldehyde metabolism or antioxidant capacity cannot be excluded. Third, the mechanistic link we propose between formaldehyde-protein adduction and parvalbumin interneuron vulnerability is inferential; direct biochemical confirmation (for example, quantification of parvalbumin protein adducts or GAD65/67 activity) was outside the scope of this study and is a natural next step. Fourth, our behavioural-anatomical correspondence, while internally consistent, remains correlative; electrophysiological confirmation of disrupted gamma oscillations or synaptic transmission would strengthen the functional claims made here. Finally, extrapolation of rodent inhalation exposure levels to real-world human occupational exposure requires caution, since dosimetry, respiratory anatomy, and exposure duration differ substantially between the two.

Conclusion

Chronic formaldehyde inhalation induces region-specific loss of parvalbumin-expressing interneurons, accompanied by oxidative stress and glial activation, in a pattern that corresponds coherently with the motor, cognitive, and affective deficits observed. These findings add cellular specificity to the existing formaldehyde neurotoxicity literature and provide an anatomical basis for renewed attention to the occupational safety of formalin use in anatomical education and practice.

Declarations

Ethics approval

All animal procedures were approved by the University of Abuja Ethics Committee for Animal Use (approval no. UAECAU/2022/0018) and conducted in accordance with the NIH Guide for the Care and Use of Laboratory Animals and European Communities Council Directive 86/609/EEC.

Funding

This work was partially supported by a joint University of Abuja, Center for Undergraduate Research grant to Abdullahi Bashir Muhammad and **Idris Nurudeen Abdullahi**

Competing interests

The authors declare that they have no competing interests.

Data availability

The datasets generated and/or analyzed during the current study are available from the corresponding author on reasonable request. All raw data, processed data, and supporting materials have been archived at the Animal Facility and Neuroscience Unit, Department of Veterinary Anatomy, University of Abuja. Due to institutional policy, the data are not publicly deposited but can be shared upon request for academic and non-commercial purposes.

Authors contributions

UIL; Conceptualization, Methodology, Validation, Writing - original draft, Writing - review & editing, Visualization, Formal analysis, Data curation, Supervision, Resources, Project administration

ABM; Methodology, Data curation, Writing - original draft, Writing - review & editing, Investigation, Visualization, Formal analysis, Resources

INA; Methodology, Data curation, Writing - review & editing, Validation, Visualization, Project administration, Formal analysis, Resources

OFO; Conceptualization, Validation, Writing - review & editing, Supervision

UEU; Investigation, Visualization, Writing - review & editing

JS; Conceptualization, Validation, Writing - review & editing, Supervision

MAA; Methodology, Data curation, Investigation, Visualization, Writing - review & editing

EEE; Conceptualization, Methodology, Validation, Visualization, Writing - original draft, Writing - review & editing

Acknowledgment

Authors are grateful for the technical support provided by staff of the Neuroscience Unit of the Department of Veterinary Anatomy, University of Abuja.

References

Akbar-Khanzadeh F, Vaquerano MU, Akbar-Khanzadeh M, Bisesi MS (1994) Formaldehyde exposure, acute pulmonary response, and exposure control options in a gross anatomy laboratory. Am J Ind Med 26:61–75.

Aslan H, Songur A, Tunc AT, Ozen OA, Bas O, Yagmurca M, Turgut M, Sarsilmaz M, Kaplan S (2006) Effects of formaldehyde exposure on granule cell number and volume of dentate gyrus: a histopathological and stereological study. Brain Res 1122:191–200.

Behrens MM, Ali SS, Dao DN, Lucero J, Shekhtman G, Quick KL, Dugan LL (2007) Ketamine-induced loss of phenotype of fast-spiking interneurons is mediated by NADPH-oxidase. Science 318:1645–1647.

Beutler E, Duron O, Kelly BM (1963) Improved method for the determination of blood glutathione. J Lab Clin Med 61:882–888.

Brown, R. E., Corey, S. C., & Moore, A. K. (1999). Differences in measures of exploration and fear in MHC-congenic C57BL/6J and B6-H-2K mice. *Behavior genetics*, *29*(4), 263-271.

Cabungcal JH, Nicolas D, Kraftsik R, Cuenod M, Do KQ, Hornung JP (2006) Glutathione deficit during development induces anomalies in the rat anterior cingulate GABAergic neurons: relevance to schizophrenia. Neurobiol Dis 22:624–637.

Cabungcal JH, Steullet P, Morishita H, Kraftsik R, Cuenod M, Hensch TK, Do KQ (2013) Perineuronal nets protect fast-spiking interneurons against oxidative stress. Proc Natl Acad Sci USA 110:9130–9135.

Cardin JA, Carlén M, Meletis K, Knoblich U, Zhang F, Deisseroth K, Tsai LH, Moore CI (2009) Driving fast-spiking cells induces gamma rhythm and controls sensory responses. Nature 459:663–667.

Chia SE, Jeyaratnam J, Ong CN, Ng TP, Lee HS (1992) Medical students' exposure to formaldehyde in a gross anatomy dissection laboratory. J Am Coll Health 41:115–119.

Coleman R (1995) Reducing the levels of formaldehyde exposure in gross anatomy laboratories. Anat Rec 243:531–533.

Costa S, Coelho P, Costa C, Silva S, Mayan O, Santos LS, Gaspar J, Teixeira JP (2008) Genotoxic damage in pathology anatomy laboratory workers exposed to formaldehyde. Toxicology 252:40–48.

Folarin, O., Olopade, F., Onwuka, S., & Olopade, J. (2016). Memory deficit recovery after chronic vanadium exposure in mice. *Oxidative Medicine and Cellular Longevity*, *2016*(1), 4860582.

Gaykema RPA, Goehler LE (2009) Lipopolysaccharide challenge-induced suppression of Fos in hypothalamic orexin neurons: their potential role in sickness behavior. Brain Behav Immun 23:926–930. doi:10.1016/j.bbi.2009.03.005.

Gerashchenko D, Kohls MD, Greco MA, Waleh NS, Salin-Pascual R, Kilduff TS, Lappi DA, Shiromani PJ (2001) Hypocretin-2-saporin lesions of the lateral hypothalamus produce narcoleptic-like sleep behavior in the rat. J Neurosci 21:7273–7283. doi:10.1523/JNEUROSCI.21-18-07273.2001.

Gurel A, Coskun O, Armutcu F, Kanter M, Ozen OA (2005) Vitamin E against oxidative damage caused by formaldehyde in frontal cortex and hippocampus: biochemical and histological studies. J Chem Neuroanat 29:173–178.

Habig WH, Pabst MJ, Jakoby WB (1974) Glutathione S-transferases: the first enzymatic step in mercapturic acid formation. J Biol Chem 249:7130–7139.

Hu H, Gan J, Jonas P (2014) Fast-spiking, parvalbumin+ GABAergic interneurons: from cellular design to microcircuit function. Science 345:1255263.

IARC (2006) Formaldehyde, 2-butoxyethanol and 1-tert-butoxypropan-2-ol. IARC Monogr Eval Carcinog Risks Hum 88:39–325.

IARC (2012) Chemical agents and related occupations: formaldehyde. IARC Monogr Eval Carcinog Risks Hum 100F:401–435.

Kann O (2016) The interneuron energy hypothesis: implications for brain disease. Neurobiol Dis 90:75–85.

Kann O, Kovács R (2007) Mitochondria and neuronal activity. Am J Physiol Cell Physiol 292:C641–C657.

Keil CB, Akbar-Khanzadeh F, Konecny KA (2001) Characterizing formaldehyde emission rates in a gross anatomy laboratory. Appl Occup Environ Hyg 16:967–972.

Kettenmann H, Hanisch UK, Noda M, Verkhratsky A (2011) Physiology of microglia. Physiol Rev 91:461–553.

Kleinnijenhuis, A. J., Staal, Y. C., Duistermaat, E., Engel, R., & Woutersen, R. A. (2013). The determination of exogenous formaldehyde in blood of rats during and after inhalation exposure. *Food and Chemical Toxicology*, *52*, 105-112.

Liu, Y., Ye, Z., Yang, H., Zhou, L., Fan, D., He, S., & Chui, D. (2010). Disturbances of soluble N-ethylmaleimide-sensitive factor attachment proteins in hippocampal synaptosomes contribute to cognitive impairment after repetitive formaldehyde inhalation in male rats. *Neuroscience, 169*(3), 1248–1254. https://doi.org/10.1016/j.neuroscience.2010.05.061

Liddelow SA, Guttenplan KA, Clarke LE, Bennett FC, Bohlen CJ, Schirmer L, Bennett ML, Münch AE, Chung WS, Peterson TC, et al. (2017) Neurotoxic reactive astrocytes are induced by activated microglia. Nature 541:481–487.

Liu, Y., Ye, Z., Yang, H., Zhou, L., Fan, D., He, S., & Chui, D. (2010). Disturbances of soluble N-ethylmaleimide-sensitive factor attachment proteins in hippocampal synaptosomes contribute to cognitive impairment after repetitive formaldehyde inhalation in male rats. *Neuroscience*, *169*(3), 1248-1254.

Misra HP, Fridovich I (1972) The role of superoxide anion in the autoxidation of epinephrine and a simple assay for superoxide dismutase. J Biol Chem 247:3170–3175.

Ohmichi K, Komiyama M, Matsuno Y, Takanashi Y, Miyamoto H, Kadota T, Maekawa M, Toyama Y, Tatsugi Y, Kohno T, Ohmichi M, Mori C (2006) Formaldehyde exposure in a gross anatomy laboratory: personal exposure level is higher than indoor concentration. Environ Sci Pollut Res Int 13:120–124.

Orsière T, Sari-Minodier I, Iarmarcovai G, Botta A (2006) Genotoxic risk assessment of pathology and anatomy laboratory workers exposed to formaldehyde by use of personal air sampling and analysis of DNA damage in peripheral lymphocytes. Mutat Res 605:30–41.

Oyagbemi, A. A., Omobowale, T. O., Asenuga, E. R., Ochigbo, G. O., Adejumobi, A. O., Adedapo, A. A., & Yakubu, M. A. (2017). Sodium arsenite-induced cardiovascular and renal dysfunction in rat via oxidative stress and protein kinase B (Akt/PKB) signaling pathway. *Redox Report*, *22*(6), 467-477.

Palomba, M., Seke-Etet, P. F., Laperchia, C., Tiberio, L., Xu, Y. Z., Colavito, V., ... & Bentivoglio, M. (2015). Alterations of orexinergic and melanin-concentrating hormone neurons in experimental sleeping sickness. *Neuroscience*, *290*, 185-195.

Percie du Sert N, Hurst V, Ahluwalia A, Alam S, Avey MT, Baker M, Browne WJ, Clark A, Cuthill IC, Dirnagl U, et al. (2020) The ARRIVE guidelines 2.0: updated guidelines for reporting animal research. PLoS Biol 18:e3000410.

Shabani M, Nazeri M, Parsania S, Razavinasab M, Zangiabadi N, Esmaeilpour K, Abareghi F (2012) Walnut consumption protects rats against cisplatin-induced neurotoxicity. Neurotoxicology 33:1314–1321. doi:10.1016/j.neuro.2012.08.004.

Sofroniew MV, Vinters HV (2010) Astrocytes: biology and pathology. Acta Neuropathol 119:7–35.

Sohal VS, Zhang F, Yizhar O, Deisseroth K (2009) Parvalbumin neurons and gamma rhythms enhance cortical circuit performance. Nature 459:698–702.

Songur A, Ozen OA, Sarsilmaz M (2010) The toxic effects of formaldehyde on the nervous system. Rev Environ Contam Toxicol 203:105–118.

Songur A, Sarsilmaz M, Ozen O, Sahin S, Koken R, et al. (2008) The effects of inhaled formaldehyde on oxidant and antioxidant systems of rat cerebellum during the postnatal development process. Toxicol Mech Methods 18:569–574.

Souza AD, Devi R (2014) Cytokinesis blocked micronucleus assay of peripheral lymphocytes revealing the genotoxic effect of formaldehyde exposure. Clin Anat 27:308–312.

Steullet P, Cabungcal JH, Coyle J, Didriksen M, Gill K, Grace AA, et al. (2017) Oxidative stress-driven parvalbumin interneuron impairment as a common mechanism in models of schizophrenia. Mol Psychiatry 22:936–943.

Steullet P, Cabungcal JH, Kulak A, Kraftsik R, Chen Y, Dalton TP, Cuenod M, Do KQ (2010) Redox dysregulation affects the ventral but not dorsal hippocampus: impairment of parvalbumin neurons, gamma oscillations, and related behaviors. J Neurosci 30:2547–2558.

Tang XQ, Zhuang YY, Zhang P, Fang HR, Zhou CF, Gu HF, Zhang H, Wang CY (2013) Formaldehyde impairs learning and memory involving the disturbance of hydrogen sulfide generation in the hippocampus of rats. J Mol Neurosci 49:140–149.

Tang, X. Q., Fang, H. R., Zhou, C. F., Zhuang, Y. Y., Zhang, P., Gu, H. F., & Hu, B. (2013). A novel mechanism of formaldehyde neurotoxicity: inhibition of hydrogen sulfide generation by promoting overproduction of nitric oxide. *PLoS One*, *8*(1), e54829.

Tong Z, Han C, Luo W, Wang X, Li H, Luo H, Zhang X, Qiang M, Zhang R, Song W, et al. (2013) Accumulated hippocampal formaldehyde induces age-dependent memory decline. Age (Dordr) 35:583–596.

Tretyakova NY, Groehler A IV, Ji S (2015) DNA-protein cross-links: formation, structural identities, and biological outcomes. Acc Chem Res 48:1631–1644.

Tulpule K, Dringen R (2013) Formaldehyde in brain: an overlooked player in neurodegeneration? J Neurochem 127:7–21.

Usende, I. L., Bintu, M. M., Daniella, O. C., Oyenike, O. A. F., Agbonu, A. O., Adedamola, A. M., ... & James, C. (2024). Neurobehavioral deficits, histoarchitectural alterations, parvalbumin neuronal damage and glial activation in the brain of male Wistar rat exposed to Landfill leachate. *Journal of Chemical Neuroanatomy*, *136*, 102377.

Usende, I. L., Leitner, D. F., Neely, E., Connor, J. R., & Olopade, J. O. (2016). The deterioration seen in myelin related morphophysiology in vanadium exposed rats is partially protected by concurrent iron deficiency. *Niger J Physiol Sci*, *31*(1), 11-22.

Usende, I. L., Olopade, J. O., Azeez, I. A., Andrioli, A., Bankole, M. O., Olopade, F. E., ... & Bentivoglio, M. (2022). Neuroecotoxicology: Effects of environmental heavy metal exposure on the brain of African giant rats and the contribution of vanadium to the neuropathology. *IBRO Neuroscience Reports*, *13*, 215-234.

Varshney R, Kale RK (1990) Effects of calmodulin antagonists on radiation-induced lipid peroxidation in microsomes. Int J Radiat Biol 58:733–743.

Vohra MS (2011) Personal formaldehyde exposure level in the gross anatomy dissecting room at College of Medicine King Saud University Riyadh. Int J Occup Med Environ Health 24:108–113.

West, M. J. (1993). New stereological methods for counting neurons. *Neurobiology of Aging, 14*(4), 275–285. doi:10.1016/0197-4580(93)90112-O

Zhang, Z., Hua, Q., & He, R. (2025). Potential Drug Interventions on Formaldehyde-Induced Neuronal Toxicity. In *Formaldehyde and Cognition* (pp. 469-499). Singapore: Springer Nature Singapore.

Zararsiz I, Kus I, Ogeturk M, Akpolat N, Kose E, Meydan S, Sarsilmaz M (2007) Melatonin prevents formaldehyde-induced neurotoxicity in prefrontal cortex of rats: an immunohistochemical and biochemical study. Cell Biochem Funct 25:413–418.

Zararsiz, I., Kus, I., Akpolat, N., Songur, A., Ogeturk, M., & Sarsilmaz, M. (2007). Protective effects of melatonin against formaldehyde-induced oxidative damage in the hippocampus of rats. *Toxicology and Industrial Health, 23*(7), 373–379.